State estimation in Medium Voltage Distribution Networks

Sai Suprabhath Nibhanupudi

Technische Universiteit Delft

TU Delft Delft University of Technology

Technolution

PHASE TO PHASE

State Estimation in Medium Voltage Distribution Networks

by

Sai Suprabhath Nibhanupudi

to obtain the degree of Master of Science

In
Electrical Engineering

at the Delft University of Technology,
to be defended publicly on Friday August 27, 2021 at 15:00

Student number:	5009685		
Project duration:	November 1, 2020 – August 27, 2021		
Thesis committee:	Dr. Anton Ishchenko,	Phase To Phase,	Company Supervisor
	Dr. S.H. (Simon) Tindemans,	TU Delft,	University Supervisor
	Prof.dr. P. (Peter) Palensky ,	TU Delft,	Graduation Committee
	Dr.ir. Aditya Shekhar,	TU Delft,	Graduation Committee

TU Delft Delft University of Technology

Technolution

PHASE TO PHASE

ABSTRACT

TRANSITION from fossil fuels to sustainable sources of energy like wind and solar is the need of the hour. All over the globe, plans are in motion to achieve this goal. This implies addition of new elements to the grid in the form of Distributed Energy Resources (DERs). These affect the working of distribution grids and to ensure reliable as well as safe operation, it is important to keep a track on the grid's state regularly which is essential to a Distribution System Operator (DSO). For this very reason, Distribution System State Estimator (DSSE) has been introduced and has been a prominent topic of interest which has been discussed in literature over the past two decades.

Because of lack in observability of the network owing to unavailability of measurements and the stochastic load profiles of the distribution network, DSSE poses its own challenges. For this very reason, it is necessary to validate the working of a suitable DSSE that is affected by the continuous changes in the grid. By selecting a suitable algorithm, this thesis attempts to solve the observability issue by introduction of pseudo-measurements.

The work in this thesis comprises of sensitivity analysis of Weighted Least Squares (WLS) algorithm tested on two networks in the Netherlands; a synthetic model of an anonymized distribution network and a part of Stedin's distribution network which has limited measuring devices data available. The percentage of pseudo-measurements is varied to determine the state estimator's accuracy. Also the statistical validity of the algorithm against measures like bias and consistency is determined with the help of scenarios generated by using Latin Hypercube Sampling (LHS).

The results obtained prove the effectiveness of the selected algorithm for DSSE and are important for the DSOs to make critical decisions when needed for grid operation.

Acknowledgements

One of the most exciting phases of my life comes to an end with this thesis. The last two years in the Netherlands has been quite eventful and and I am grateful for all the experiences I have had. With the global pandemic around, it indeed was a challenging journey.

I would like to offer my sincere gratitude to my supervisor Dr. Anton Ishchenko at Phase to Phase BV for providing me with the opportunity as well as guiding me throughout the entire course of the project. Also, I would like to thank my TU Delft supervisor Dr. Simon Tindemans for his valuable inputs in the weekly meetings and the patience he has shown towards me. I would also like to thank Dr. Peter Palensky and Dr. Aditya Shekhar for accepting to be a part of my graduation committee.

Additionally, I would like to thank everyone at Phase to Phase and Technolution for making me feel welcome over the duration of my thesis. I would also like to thank Bart Kers from Stedin and Aykut Uysal from Enexis for the networks and measurement data provided. Due to the time constraints, the data from Enexis has not been used in this thesis but will definitely be used in the future.

I consider myself fortunate to have crossed paths with quite a few influential individuals and forge friendships over the years. I would like to thank all my friends in the Netherlands as well as the others spread across the globe and back home in India for being instrumental in my journey so far.

This journey would of course have not been possible without the unending support and sacrifices from my family especially my parents and grandparents all throughout my life. I would have loved to share the stories and interesting challenges I experienced with my beloved grandfather who passed away during my student journey.

Entering the next phase of life, I am excited for the endless opportunities and hopefully many life-changing experiences that lie ahead. I am looking forward to contribute my learnings as an engineer in the future.

Wishing you a pleasant reading!

Sai Suprabhath Nibhanupudi
Delft, August 2021

Contents

List of Figures

List of Tables

ABBREVIATIONS

DER Distributed Energy Resource

DMS Distribution Management System

DSSE Distribution System State Estimator

DSO Distribution System Operator

ALPG Artificial Load Profile Generator

SCADA Supervisory Control and Data Acquisition

WLS Weighted Least Squares

LMS Least Median of Squares

LTS Least Trimmed Squares

LAV Least Absolute Value

GM Generalized Maximum Likelihood

AMI Advanced Metering Infrastructures

AMR Automated Meter Reading

PF Power Flow

MV Medium Voltage

LV Low Voltage

DSM Demand Side Management

RTU Remote Terminal Unit

PLC Programmable Logic Controller

HMI Human Machine Interface

LHS Latin Hypercube Sampling

Vision NA Vision Network Analysis

1

Introduction

The first chapter gives a general overview about the rapidly changing energy scenario and why state estimation is needed to keep the grid in check. The problem definition of the thesis is then discussed along with the research questions. The significance and the structure of a DSSE are discussed. The chapter ends with an outline of the thesis.

1.1. Motivation

The fast paced technological advancements by the human race over the past few decades has come at the cost of a deteriorating environment. Usage of fossil fuels as the main source of electricity production over this time is one of the most pressing factors. Therefore, in order to get back to a sustainable way of life, renewable sources of energy are being resorted to as an alternative and serve as the perfect replacement to fossil fuels [1]. Over the past few years, it is seen that the energy demand is increasing rapidly and with this, a switch to renewable sources to produce electricity is picking up too. It is estimated that by the year 2050, nearly 86% of electricity generation in the world will be satisfied by renewables of which 60% is accounted by photovoltaics and wind [2]. This means the penetration into the existing grid with newer technologies is increasing. Netherlands is one of the leading countries around the world promoting this shift. A detailed plan has been laid out to achieve this transition by the government of Netherlands [3]. Electric Mobility and solar panel generation are two sustainable aspects being promoted at large. The country is also involved in the North Sea Wind Power Hub project which aims to create a large offshore wind power hub for this very reason of achieving 100% transition to sustainable electricity [4].

The inclusion of these DERs in the power system network affects the voltage profiles, quality of power and cause many other issues related to grid protection [5]. For

this very reason, more control aspects have to be introduced to the grid. This requires constant monitoring at a Distribution Management System (DMS). State estimation is the heart of a DMS and helps to determine the state estimates using State Estimation algorithms. The output from the estimator enables to further perform important functions like security and contingency analysis. This in turn helps in monitoring and having control over most of the devices like circuit breakers, switches and so on in the substation.

Phase to Phase BV is a company located in the Netherlands that provides software solutions for power utilities, industry and engineering firms to help in grid planning and design. Most of the Dutch DSOs (like Alliander, Stedin etc.) use these products: Vision Network Analysis (Vision NA) for high & medium voltage networks and Gaia LV Network Design for Low Voltage (LV) networks. The developed prototype of state estimation as part of this thesis serves as a foundation for the module to be implemented in Vision NA for commercial usage.

1.2. DISTRIBUTION SYSTEM STATE ESTIMATION

The components of the DSSE block and their functions in a DMS are described here briefly [6]. The basic structure of the DSSE block is shown in figure 1.1.

1.2.1. NETWORK DATA

This is the data of the topology of network, line impedances, line charging susceptances, transformer data and so on.

1.2.2. MEASUREMENTS

The measurements available in a distribution system fall rather short in terms of requirement to make the network observable. Based on the availability and type of measurements, they are essentially classified into three types namely: **Real**, **Virtual** and **Pseudo** measurements.

- **Real Measurements:** These are the telemetered measurements which are obtained for the measurement points in the grid. Voltage magnitudes, power injections, power flows and branch currents are included in this.
- **Virtual Measurements:** These are very accurate and deterministic (the nodes with no loads). The zero injections in the buses come under this type.
- **Pseudo Measurements:** These are the measurements computed without any data from telemetering. These are necessary to make the system observable. These are derived using historical data and various customer data if available.

1.2.3. MEASUREMENT VARIANCES

As the state estimation is performed statistically, it is important to have variances data as input. The telemetered measurements have variances based on the accuracy of equipment. For the virtual measurements, the variance is low. The pseudo measurements are modelled with high variances because of the uncertainty present.

1.2.4. STATE ESTIMATION

The primary objective of a state estimation algorithm is to estimate the states of the system with the available data.

1.2.5. OUTPUTS

The output of the state estimation block is needed for various control and operating tasks in a Distribution System. The outputs here are the voltage magnitudes and angles.

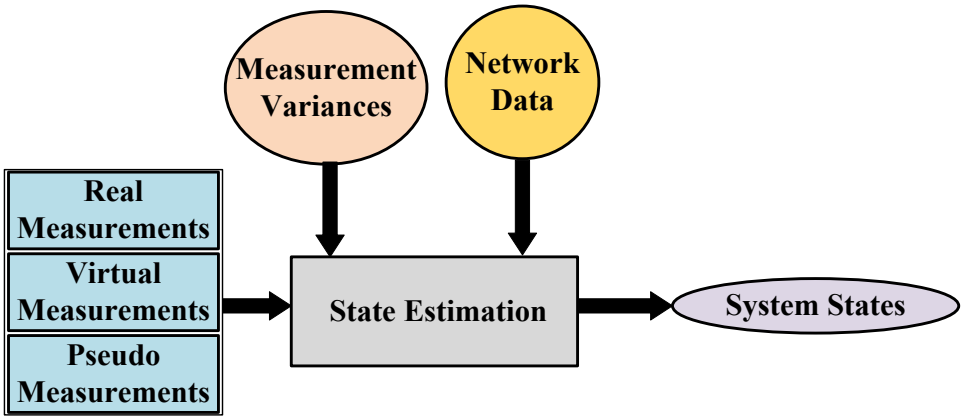

Figure 1.1: DSSE Functional Block

1.3. OBJECTIVE & RESEARCH QUESTIONS

This thesis aims to develop a working prototype of a state estimator which explores a feasible method of formulating pseudo measurements based on load probability density function approach with the help of historical data for any network configuration – including non-radial topologies where most existing methodologies cannot be applied. The developed algorithm is to be applied on Dutch Medium Voltage (MV) distribution networks which are characterized by underground cables rather than overhead lines and high load concentrations due to high population density in the Netherlands com-

pared to the other countries. The research done so far on state estimation of such networks is quite limited.

The research questions that need to be answered to achieve this goal are:

- Which State Estimation Method(s) are suitable to be applied for the distribution networks across the Netherlands?
- How to adapt the state estimation algorithm selected for distribution grids?
- What are the mathematical assumptions to be considered in order to formulate the pseudo measurements?
- How does the state estimation algorithm perform with varying levels of redundancy in measurements?

1.4. RESEARCH APPROACH AND TOOLS

- **Thesis Scope**
  The first and foremost step of the project is to identify the research outcomes keeping in mind the research questions to be answered.
- **Literature Review**
  After the identification of the scope, literature review is performed in previous studies regarding the various algorithms employed for distribution system state estimation as well as formulation of pseudo-measurements. This allows to paint a clear picture on the research that needs to be done.
- **Model Setup**
  The test network is selected and designed in Vision NA whose data is imported to MATLAB as a Matpower file to first test the working in both the tools.
- **Modelling of measurements**
  Load scenarios are created for the test network based on the rating of transformers using an Artificial Load Profile Generator (ALPG) tool developed in Python [7], [8].
- **Sensitivity analysis**
  The imported network in MATLAB along with the generated measurements are used to create multiple loading scenarios and see their effect on the state variables.
- **Conclusions**
  The results obtained are evaluated against the research questions mentioned and further scope is discussed.

1.5. SCIENTIFIC CONTRIBUTIONS

State estimation in distribution networks is being looked onto in the past few years which is critical for power system planning and operation. The thesis develops test models from Dutch DSOs. The topology, length of cables and load profiles are based on the networks in Netherlands which have a distinctive structure (underground cables). Underground cables are characterized by much higher shunt capacitances and have different parameters compared to overhead lines. The conclusions from this thesis are applicable to most of the other distribution networks in the Netherlands. Further, Vision NA software developed by Phase to Phase BV is used along with MATLAB as part of the thesis.

Sensitivity Analysis is performed on the test networks to evaluate the assumptions taken and draw further conclusions. The different scenarios considered gives a basic overview of the working of a Dutch Distribution network. With the increasing DERs in the network, and the advancement of metering technologies as well as the stochastic nature of the load profiles, the DSOs need to evolve from the classical load flow studies to the alternate method of state estimation to make short term planning decisions. The results obtained can be further validated and a module for State Estimation is planned to be included in Vision NA which helps the DSOs to use the feature on their networks.

1.6. THESIS OUTLINE

Chapter 1 gives introduction for the thesis. The background and research objectives are described. The approach followed for this thesis is described in detail and contributions from this thesis are mentioned.

Chapter 2 delves into the literature study of the various algorithms implemented which are suitable for a DSSE.

Chapter 3 describes the State Estimation Algorithm implemented. The modelling of the network as well as the algorithm is explained mathematically.

Chapter 4 gives a basic outlook on a typical Dutch MV network and the study networks considered in this thesis.

Chapter 5 explains the modelling of the different kinds of measurements and the ALPG tool used.

Chapter 6 discusses the results obtained from the analysis done on the test network systems.

Chapter 7 gives the conclusion of the thesis and further recommendations to this research work.

2

Literature Review

The majority of the power distribution system networks were built in the early 1950s. Over time, the demand of electricity as well as complexity of the grid has seen an increase. This is due to a shift in energy requirements and an increased traction in local energy production. The concept of prosumers is also encouraging customers to install small sources of energy in their homes. This leads to the conclusion that the distribution grid is vulnerable than before and needs continuous monitoring to keep it up and running all the time. To overcome the inflexibility of power flow, Schweppe [9]–[11] introduced State Estimation as an alternate method to classical load flow first in transmission systems. Recently, various researchers have been working on state estimation in distribution networks. The overview of the network can be determined with the help of a state estimator which receives measurement data from the DMS like Supervisory Control and Data Acquisition (SCADA) system that collects and analyses near real-time distribution network information. Based on the determined state of the network, actions regarding security and contingency analysis as well as monitoring of substation equipment like circuit breakers, switches and many more are further taken. The major differences of state estimation in transmission and distribution networks is explained in Section 2.1.

2.1. Transmission vs Distribution State Estimation

A stark contrast between the transmission and distribution network state estimation is the structure of networks and availability of measurements. Firstly, the operation of distribution networks is mostly radial. Secondly, in transmission systems the redundancy of measurements makes state estimation of networks rather easier inspite of presence of bad data. Also, distribution networks are characterized with shorter lines and higher R/X ratios connected to rather uneven loads with minimal or no redundancy in measurements. Limited monitoring of the network is a challenge in the case of distribution networks. The fact that available measurements are

limited led to the introduction of pseudo-measurements which are filled in to make the overall system observable and thus perform state estimation. Formulation of pseudo-measurements is done using the historical data and customer data if available using correlation approach or load probability density function approach [12]. These pseudo-measurements have higher uncertainty which leads to larger variance in the formulated measurements. Therefore a suitable algorithm should be selected that is capable of handling such uncertainty in measurements.

2.2. DSSE Algorithms

In the past twenty years, the concept of DSSE has been in focus due to the increasing uncertainty caused by the integration of DERs in the grid. The most conventional method for state estimation is the WLS Method.

Over time, the measurements provided by SCADA degrade due to systemic errors. This occurs mainly due to the instrument not being calibrated which is due to environmental factors such as weather and temperature. This leads to an introduction of bias in the power measurements. These are called bad data. In statistics, bias analysis has been of importance for quite some stime now. In [13], Rousseeuw explored various types of estimators using various objective functions. Basing this, various mathematical formulations have been proposed to further increase the robustness of the system in the event of facing bad data (outliers) which are discussed briefly. All these formulations consider the measurement function as $\mathbf{h}$ and the state vector $\mathbf{x}$ which is connected to the measurement vector $\mathbf{z}$ as shown in equation (2.1) where $\mathbf{r}$ is the residual or the error measurement vector.

$$\mathbf{z} = h(\mathbf{x}) + r \tag{2.1}$$

2.2.1. Weighted Least Squares Method

The WLS method is very widely used. The main objective is to minimise the sum of squares of the residuals as shown in equation (2.2).

$$\underset{\mathbf{x}}{\text{Minimise}} : \sum_{j=1}^{n} r_j^2(\mathbf{x}) \quad \text{where} \quad r_j(\mathbf{x}) = z_j - h_j(\mathbf{x}) \tag{2.2}$$

Further improvements have been done by replacing the objective function in WLS to increase the robustness at the cost of computational efficiency.

2.2.2. Least Median of Squares Method

Least Median of Squares (LMS) algorithm is not sensitive to outliers or the bad data [14]. Instead of the conventional way of minimizing the sum of squares of residuals,

the median of the squares of residuals is minimized as shown in equation (2.3).

$$\underset{\mathbf{x}}{\text{Minimise}} : median(r_1^2(\mathbf{x}), r_2^2(\mathbf{x}), ..., r_n^2(\mathbf{x})) \tag{2.3}$$

In [15], this algorithm is used to identify the outliers which is made easier using a power system decomposition methodology which is the process of breaking down the overall system into smaller subsystems and applying the algorithm to minimize the outliers effect.

2.2.3. LEAST TRIMMED SQUARES METHOD

Instead of performing the least squares method over the entire dataset, a subsystem is considered which contains $\boldsymbol{k}$ of the $\boldsymbol{n}$ points [15] as shown in equation (2.4). The $\boldsymbol{n}$-$\boldsymbol{k}$ points do not affect the fit considered. This method is called Least Trimmed Squares (LTS). Similar to LMS, considering a subsystem enables to have lesser effect of the outliers on the final output.

$$\underset{\mathbf{x}}{\text{Minimise}} : \sum_{j=1}^{k} r_j^2(\mathbf{x}) \tag{2.4}$$

2.2.4. LEAST ABSOLUTE VALUE METHOD

Least Absolute Value (LAV) is another very robust method which is very efficient in bad data rejection [16] represented in equation (2.5). The LAV algorithm is vulnerable when leverage measurements or points are present [17]. These refer to the values which act abnormal in an already sparse Jacobian Matrix.

$$\underset{\mathbf{x}}{\text{Minimise}} : \sum_{j=1}^{n} | r_j(\mathbf{x}) | \tag{2.5}$$

2.2.5. GENERALIZED MAXIMUM LIKELIHOOD

To overcome the vulnerability of leverage points, Generalized Maximum Likelihood (GM) algorithm has been introduced [18] represented by equations (2.6) and (2.7).

$$\underset{\mathbf{x}}{\text{Minimise}} : \sum_{j=1}^{n} \sigma_j^{-2} \rho(r_{S_j}(\mathbf{x})) \tag{2.6}$$

$$\rho\left(r_{S_j}\right) = \begin{cases} \dfrac{1}{2} r_{S_j}^2(\mathbf{x}), \text{ for } \left|r_{S_j}\right| < c \\ c\left|r_{S_j}(\mathbf{x})\right| - c^2/2, \text{ elsewhere} \end{cases} \tag{2.7}$$

where $\boldsymbol{c}$ is the breakpoint to balance robustness (generally between 1.5 and 3) shown by Huber [19] and $\boldsymbol{\sigma_j}$ is calculated with the help of bad data detection threshold and projection statistics [18]. r_{S_j} is the standardized residual. The basic purpose of this algorithm is to bound the influence of the outlier by using a weight or in this case standardizing the residual [13].

The robustness of these algorithms is tested in [20] considering various factors like measurement uncertainty and change in measurement redundancy. From this, the advantages and disadvantages of these algorithms have been tabulated in table 2.1.

Table 2.1: Comparision of algorithms [21]

Algorithm	Advantages	Disadvantages
Weighted Least Squares	• Simple, widely used.	• Fails in presence of bad data.
Least Median of Squares	• Robust against bad data.	• Requires high redundancy of measurements.
Least Trimmed Squares	• Robust against bad data.	• High memory requirement.
Least Absolute Value	• Robust against bad data	• High cost in computation. • Sensitive to measurement uncertainty.
Generalized Maximum Likelihood	• Robust against bad data.	• Sensitive to parameter selection.

LMS and LTS algorithms are centered around the concept of creating subsystems from the given grid which requires a lot of memory to be used since a lot of iterations has to be done multiple times to get the clear overall picture. LAV algorithm is very sensitive to measurement uncertainty and this poses a major problem in distribution networks where definite values are hard to come by.

The GM algorithm is posed with the problem of uncertainty over convergence as and when the parameters used as input are changed. Overall; LMS, LTS, LAV and GM algorithms though robust against bad data lack efficiency in dealing with the high uncertainty in measurements and are computationally uneconomical. Also a good estimator needs to satisfy the condition of bias which refers to the mean of the error estimate to be zero and be consistent which implies that the error estimate statistically corresponds to the measurement error variance. For this very reason, WLS method is best suitable for state estimation studies and is widely used assuming

there is no bad data [22].

2.3. WEIGHTED LEAST SQUARES FORMULATIONS

The differences between transmission and distribution systems also changes the way DSSE algorithm is formulated. Depending on the availability of measured variables and the choice of Power Flow (PF) (AC or DC), the Measurement Jacobian is formulated. Many types of formulations are available in literature. Two of the most used ones are the Voltage based and Branch Current based DSSE approaches.

2.3.1. VOLTAGE BASED APPROACH

In transmission systems, the state variables generally considered are the bus voltage magnitudes and bus angles. A similar approach is employed in DSSE too.

In [23], Baran and Kelly use WLS method based on three phase voltage node formulation. The implemented method can handle power injections, voltages as well as branch currents as measurements.

In [24], the authors implement a linearized, three-phase estimator for smart distribution system applications. There is scope for inclusion of synchronized phasor measurements in the implemented algorithm.

Another method has been proposed by Youman Deng and others in [25], where the traditional WLS estimation method is decomposed into multiple WLS subproblems which eliminates the need of a sparse matrix. This algorithm has been tested on a practical distribution system in China.

2.3.2. CURRENT BASED APPROACH

A few other works have considered branch currents as state variables too and are explained here briefly.

In [26], the authors have proposed a three-phase current based state estimator. All the measurements (voltage, power and current) are converted to their current equivalents and the corresponding Jacobians are calculated.

In [27], the authors consider branch currents as state variables and the method is seen to be efficient in weakly meshed and radial networks. To make computation easier, the network is reduced by considering individual feeders and assuming the loads are uniformly distributed. This method is further improved to take into consideration the Advanced Metering Infrastructures (AMI) [28].

In [29], a current based formulation is implemented with voltage magnitudes as

measurements. This is done in order to improve the accuracy of the state estimator with the possible availability of voltage magnitudes from measuring devices at the distribution level.

In [30], the authors present a three-phase DSSE based on branch current approach. This algorithm uses the data from Automated Meter Reading (AMR) to estimate transformer loads in the distribution system which are used as pseudo-measurements.

Table 2.2: Comparision of the two approaches for WLS method [21]

Parameter/Approach	Voltage based	Current based
Fast Convergence	✓	×
State independent Jacobian	✓	×
Low sensitivity to network impedance	✓	×
Small angle difference assumption	✓	✓
Good performance on non-radial topologies	✓	×

The two approaches are compared in table 2.2. It is observed that from literature, a faster convergence is observed in voltage based approach than in a current based approach. One other factor that stands out in favour of the voltage based approach is having the Jacobian matrix being independent to the states as compared to the current based approach. The performance on all kinds of networks and sensitivity towards network impedance are in the favour of voltage based approach. Considering all these factors, the voltage based WLS approach is the clear choice.

2.4. MODELLING OF PSEUDO-MEASUREMENTS

In DSSE, the lack of real measurement data forces it to rely on pseudo-measurements which generally originate from standard load profiles [31]. The impact of pseudo-measurements on state estimation is very high and availability of more information about the behaviour of profiles can help in accurate modelling.

Using a correlation approach or a load probability density function approach, modelling of pseudo-measurements can be done as explained in [12].

Based on customer billing data and the historical meter data available, many statistical methods have been employed to model the load data. Usage of neural network approach to model load profiles in distribution networks is explored in [32]. The researchers suggest the use of synthetic data with defined customer classes as a way to improve load forecast modelling.

Another approach is to find the most probable value which is the mean for uni-modal distributions that is applicable here and the standard deviation of the power

injections for time resolutions considered based on the synthesized load profiles or the available bottom up approach profiles. This is based on the load probability density function approach where the profiles are considered to be simple Gaussian models and hence the corresponding values are obtained [12]. In order to fill the gaps created due to the absence of pseudo-measurements, these most probable values can be utilised to achieve an observable network for state estimation.

The DSOs generally use loadflow calculations for their short-term planning studies which are typically based on analysis of past situations. Previously, the only available measurement at the transformer loads is the maximum absolute value of current but not the exact moment it occurred (which is mostly different for different transformer loads). Over time, with the presence of more loads in the network, and the increase in complexity along with technological advancements in the meters, different type of measurements have become available. In larger networks, the classical load flow technique is inefficient owing to the fact that the exact values of power injections are unavailable at all the loads which are required to solve the problem. This opens up new avenues to further improve the handling of data using the state estimation algorithm and pseudo-measurements play an important role here to fill up the missing gaps (measurements) as mentioned previously.

The general approach is to model the pseudo-measurements through a normal distribution owing to its compatibility with WLS algorithm which is used here for the data that is modelled synthetically. For residential households which account to more than 50 in a neighbourhood, it is shown that the central limit theorem is valid for the overall load profiles provided that there is no correlation in the random variables (in this case the powers of households). Considering this, a normal distribution is assumed [33].

Synthesizing residential load profiles has been concentrated upon by many researchers and in fact few of them have also developed tools for the same [7], [34]–[36]. Various time resolutions are taken into account to generate the profiles in different bottom up approaches. In order to generate more realistic profiles, it is essential to identify required datasets such as occupancy of households, the solar irradiation data and possible penetration of DERs into the grid.

With the help of this profile data, the mean and variances for different instances of time are documented and these are used as pseudo-measurement data when needed.

3

Weighted Least Squares Method

Many state estimation techniques have been proposed by researchers over a long period of time. The main purpose of state estimation technique is to make sure that the power system is in a normal operating state always. Here, the WLS Method is chosen. The assumptions made as part of this thesis are as follows:

- **State Variables:** The bus voltages and angles are considered as the state of the system which have to be calculated
- **Measurements:** The real and reactive power injections as well as the real and reactive power flows along with bus voltage magnitudes and magnitude of current flows are considered.
- **Bad Data:** It is assumed that no bad data has to be processed considering the large variances created due to the pseudo-measurements already in place.

3.1. Mathematical Modelling of the Network

The modelling of the entire WLS Estimation algorithm is explained in detail and this entire section is based upon [37].

3.1.1. Network considered

The power system is assumed to be balanced and in steady state conditions. This in turn means that the loads and power flows in branches are three phase and balanced. The series and shunt devices considered are symmetrical and balanced in

three phases. With all these considerations, it is therefore possible to model the entire power system using single phase positive sequence equivalent circuit.

Network Branch Modelling

The lines are represented with a two-port π model whose parameters correspond to that of a positive sequence equivalent circuit with nodes ***m*** and ***n***. The admittance of the line is considered to be $\mathbf{G_{mn} + jB_{mn}}$ and the line charging susceptance is **j2B** where ($B_m = B_n = B$) are the corresponding per phase shunt capacitances of the buses and shunt conductances G_m & G_n. The circuit is shown as below in figure 3.1.

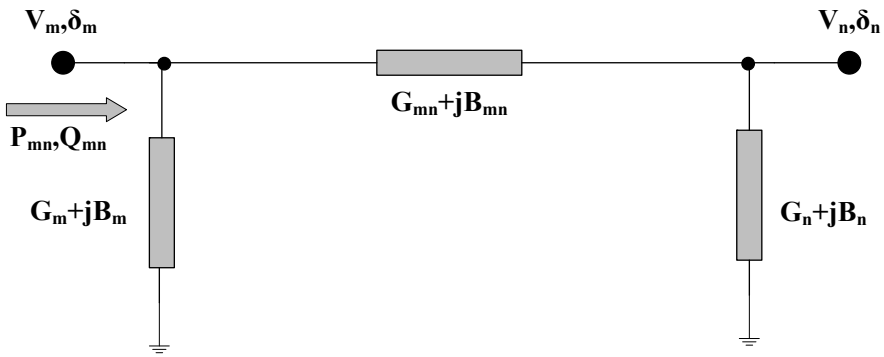

Figure 3.1: Two port π Model Network

3.1.2. LOADS AND GENERATIONS

The loads and generations are modelled as real and reactive power injections at the terminals. The consumption is represented by negative power injections and the generation is represented by positive current injections.

3.1.3. TRANSFORMER MODEL

Off-nominal but in phase taps of transformers can be modeled as ideal transformers in series with the line impedances as shown in figure 3.2. The two bus terminals of the transformer are **m** and **n** known as tap-side side and impedance side bus respectively. **a** is the tap ratio of the transformer.

The impedance of the line **p-n** is $R + jX$. The admittance is considered to be **y**. The nodal equations for the figure 3.2 are derived as shown in equation (3.1)-equation (3.3).

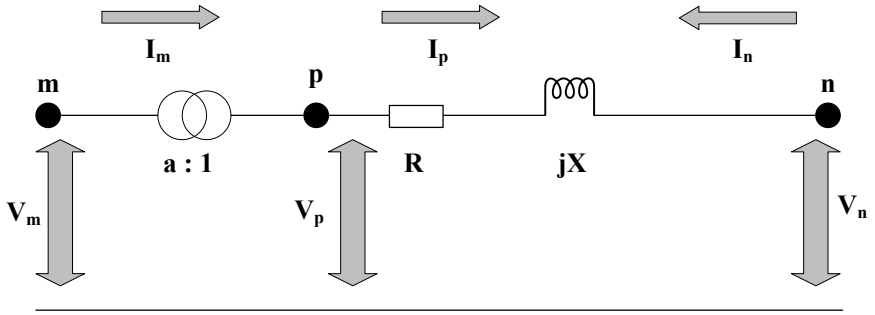

Figure 3.2: Transformer model

The terminal current injections in line **p-n** are given by equation (3.1).

$$\begin{bmatrix} I_p \\ I_n \end{bmatrix} = \begin{bmatrix} y & -y \\ -y & y \end{bmatrix} \begin{bmatrix} V_p \\ V_n \end{bmatrix} \tag{3.1}$$

The equivalent two port circuit for the equation (3.1) - equation (3.3) is shown in figure 3.3.

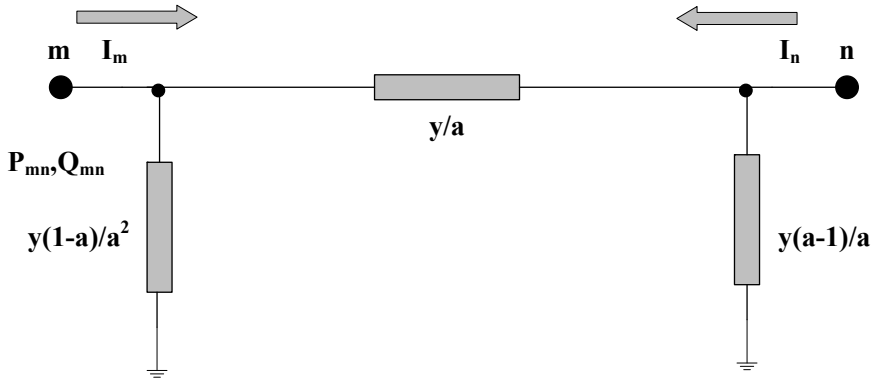

Figure 3.3: Two port equivalent Transformer circuit model

Substitution of I_p and V_p as shown in equation (3.2) gives equation (3.3).

$$\begin{aligned} I_p &= a \cdot I_m \\ V_p &= V_m / a \end{aligned} \tag{3.2}$$

$$\begin{bmatrix} I_m \\ I_n \end{bmatrix} = \begin{bmatrix} y/a^2 & -y/a \\ -y/a & y \end{bmatrix} \begin{bmatrix} V_m \\ V_n \end{bmatrix} \tag{3.3}$$

3.1.4. ADMITTANCE MATRIX

The figure 3.3 can be used to model the admittance matrix of the entire network using Kirchhoff's current law at each of the buses as shown in equation (3.4). The admittance matrix in general is complex and very sparse. It is also symmetric in nature.

$$\mathbf{I} = \begin{bmatrix} I_1 \\ I_2 \\ \vdots \\ I_N \end{bmatrix} = \begin{bmatrix} Y_{11} & Y_{12} & \cdots & Y_{1N} \\ Y_{21} & Y_{22} & \cdots & Y_{2N} \\ \vdots & \vdots & \vdots & \vdots \\ Y_{N1} & Y_{N2} & \cdots & Y_{NN} \end{bmatrix} \begin{bmatrix} V_1 \\ V_2 \\ \vdots \\ V_N \end{bmatrix} = \mathbf{Y} \cdot \mathbf{V} \tag{3.4}$$

where

$\mathbf{I}$	:	Vector of current injections,
$\mathbf{Y_{mn}}$	:	$(m,n)^{th}$ element,
$\mathbf{V}$	:	Voltage phasors vector

3.1.5. MEASUREMENT VECTOR MODELLING

The state vector consisting of voltages and angles is denoted by $\mathbf{x}$. The measurement vector which is non-linear relating the state vector and the measurement vector is considered as in equation (3.5) :

$$z = \begin{bmatrix} z_1 \\ z_2 \\ \vdots \\ z_m \end{bmatrix} = \begin{bmatrix} h_1(x_1, x_2, \ldots, x_n) \\ h_2(x_1, x_2, \ldots, x_n) \\ \vdots \\ h_m(x_1, x_2, \ldots, x_n) \end{bmatrix} + \begin{bmatrix} e_1 \\ e_2 \\ \vdots \\ e_m \end{bmatrix} = \mathbf{h(x)} + \mathbf{e} \tag{3.5}$$

where

$\mathbf{x}$	:	System states (voltages and angles) vector,
$\mathbf{e}$	:	Measurement errors vector,
$\mathbf{h(x)}$	:	Vector of functions corresponding to non-linear measurements.

The following assumptions are made as part of implementation of this algorithm:

- $\mathbf{e}$ is Gaussian noise with zero mean represented by equation (3.6).

$$e = N(0, R) \tag{3.6}$$

- The error measurements are assumed to be independent of each other.

R is the error covariance measurement matrix given by equation (3.7) where the measurements are assumed to be independent of each other and σ_{zm}^2 is the variance of the m^{th} measurement. The total number of measurements are $\boldsymbol{k}$.

$$\mathbf{R} = \text{diag}\{\sigma_{z1}^2, \sigma_{z2}^2, \ldots, \sigma_{zm}^2\} \tag{3.7}$$

The first bus is considered to be slack bus, therefore its angle is assumed to be zero for reference. The state vector therefore is represented by equation (3.8) where δ_m and V_m are the angle and voltage of the m^{th} bus respectively.

$$\mathbf{x} = \begin{bmatrix} \delta_2 \\ \vdots \\ \delta_n \\ \\ V_1 \\ \vdots \\ V_n \end{bmatrix} \tag{3.8}$$

3.1.6. MEASUREMENT FUNCTIONS

Typically, the power flows between the lines, the active and reactive power injections, the bus voltage magnitudes as well as the branch currents are the measurements considered. These measurements can be represented in either polar or rectangular form depending on the convenience. Not all measurements need to be considered if the system is observable with few of these provided. The equations (3.9) to (3.14) are modelled with respect to figure 3.1 [38].

Line Power Flows

Active and reactive power flows between buses $\boldsymbol{m}$ and $\boldsymbol{n}$:

$$P_{mn} = V_m^2 (G_{mn} + G_m) - V_m V_n (G_{mn} \cos\delta_{mn} + B_{mn} \sin\delta_{mn}) \tag{3.9}$$

$$Q_{mn} = -V_m^2 (B_{mn} + B_m) - V_m V_n (G_{mn} \sin\delta_{mn} - B_{mn} \cos\delta_{mn}) \tag{3.10}$$

Power injections

Real and reactive power injections at bus $\boldsymbol{m}$:

$$P_m = \sum_{n \in \mathcal{N}_m} P_{mn} = V_m \sum_{n \in \mathcal{N}_m} V_n (G_{mn} \cos\delta_{mn} + B_{mn} \sin\delta_{mn}) \tag{3.11}$$

$$Q_m = \sum_{n \in \mathcal{N}_m} Q_{mn} = V_m \sum_{n \in \mathcal{N}_m} V_n (G_{mn} \sin\delta_{mn} - B_{mn} \cos\delta_{mn}) \tag{3.12}$$

Branch Currents

The branch current between buses $\boldsymbol{m}$ and $\boldsymbol{n}$:

$$I_{mn} = \frac{\sqrt{P_{mn}^2 + Q_{mn}^2}}{V_m} \tag{3.13}$$

Ignoring the shunt admittance jB, the equation is simplified as:

$$I_{mn} = \sqrt{\left(G_{mn}^2 + B_{mn}^2\right)\left(V_m^2 + V_n^2 - 2V_{im}V_n\cos\delta_{mn}\right)} \tag{3.14}$$

3.1.7. MEASUREMENT JACOBIAN

The Jacobian measurement matrix **H** with the measurement functions considered is given in equation (3.15). It is non-linear. The first derivatives with respect to system states are taken and computed by linearizing with respect to the Weighted Least Squares Algorithm and is based on [37].

$$\mathbf{H} = \begin{bmatrix} \frac{\partial V_{mag}}{\partial \delta} & \frac{\partial V_{mag}}{\partial V} \\ \frac{\partial P_{inj}}{\partial \delta} & \frac{\partial P_{inj}}{\partial V} \\ \frac{\partial Q_{inj}}{\partial \delta} & \frac{\partial Q_{inj}}{\partial V} \\ \frac{\partial P_{flow}}{\partial \delta} & \frac{\partial P_{flow}}{\partial V} \\ \frac{\partial Q_{flow}}{\partial \delta} & \frac{\partial Q_{flow}}{\partial V} \\ \frac{\partial I_{mag}}{\partial \delta} & \frac{\partial I_{mag}}{\partial V} \end{bmatrix} \tag{3.15}$$

Jacobians corresponding to **voltage magnitude** measurements:

$$\frac{\partial V_m}{\partial V_m} = 1 \tag{3.16}$$

$$\frac{\partial V_m}{\partial V_n} = \frac{\partial V_m}{\partial \delta_m} = \frac{\partial V_m}{\partial \delta_n} = 0 \ (m \neq n) \tag{3.17}$$

Jacobians corresponding to **active power injection** measurements:

$$\frac{\partial P_m}{\partial \delta_m} = \sum_{n=1}^{N} V_m V_n \left(-G_{mn}\sin\delta_{mnj} + B_{mn}\cos\delta_{mn}\right) - V_m^2 B_m \tag{3.18}$$

$$\frac{\partial P_m}{\partial \delta_n} = V_m V_n (G_{mn} \sin \delta_{mn} - B_{mn} \cos \delta_{mn}) \tag{3.19}$$

$$\frac{\partial P_m}{\partial V_m} = \sum_{n=1}^{N} V_n (G_{mn} \cos \delta_{mn} + B_{mn} \sin \delta_{mn}) + V_m G_m \tag{3.20}$$

$$\frac{\partial P_m}{\partial V_n} = V_m (G_{mn} \cos \delta_{mn} + B_{mn} \sin \delta_{mn}) \tag{3.21}$$

Jacobians corresponding to **reactive power injection** measurements:

$$\frac{\partial Q_m}{\partial \delta_m} = \sum_{n=1}^{N} V_m V_n (G_{mn} \cos \delta_{mn} + B_{mn} \sin \delta_{mn}) - V_m^2 G_m \tag{3.22}$$

$$\frac{\partial Q_m}{\partial \delta_n} = V_m V_n (-G_{mn} \cos \delta_{mn} - B_{mn} \sin \delta_{mn}) \tag{3.23}$$

$$\frac{\partial Q_m}{\partial V_m} = \sum_{n=1}^{N} V_n (G_{mn} \sin \delta_{mn} - B_{mn} \cos \delta_{mn}) - V_m B_m \tag{3.24}$$

$$\frac{\partial Q_m}{\partial V_n} = V_m (G_{mn} \sin \delta_{mn} - B_{mn} \cos \delta_{mn}) \tag{3.25}$$

Jacobians corresponding to **real power flow** measurements:

$$\frac{\partial P_{mn}}{\partial \delta_m} = V_m V_n (G_{mn} \sin \delta_{mn} - B_{mn} \cos \delta_{mn}) \tag{3.26}$$

$$\frac{\partial P_{mn}}{\partial \delta_n} = -V_m V_n (G_{mn} \sin \delta_{mn} - B_{mn} \cos \delta_{mn}) \tag{3.27}$$

$$\frac{\partial P_{mn}}{\partial V_m} = -V_n (G_{mn} \cos \delta_{mn} + B_{mn} \sin \delta_{mn}) + 2(G_{mn}) V_m \tag{3.28}$$

$$\frac{\partial P_{mn}}{\partial V_n} = -V_m (G_{mn} \cos \delta_{mn} + B_{mn} \sin \delta_{mn}) \tag{3.29}$$

Jacobians corresponding to **reactive power flow** measurements:

$$\frac{\partial Q_{mn}}{\partial \delta_m} = -V_m V_n (G_{mn} \cos \delta_{mn} + B_{mn} \sin \delta_{mn}) \tag{3.30}$$

$$\frac{\partial Q_{mn}}{\partial \delta_n} = V_m V_n (G_{mn} \cos \delta_{mn} + B_{mn} \sin \delta_{mn}) \tag{3.31}$$

$$\frac{\partial Q_{mn}}{\partial V_m} = -V_n (G_{mn} \sin \delta_{mn} - B_{mn} \cos \delta_{mn}) - 2V_m (B_{mn} + B_m) \tag{3.32}$$

$$\frac{\partial Q_{mn}}{\partial V_n} = -V_m (G_{mn} \sin \delta_{mn} - B_{mn} \cos \delta_{mn}) \tag{3.33}$$

Jacobians corresponding to **branch current** measurements:

$$\frac{\partial I_{mn}}{\partial \delta_m} = \frac{G_{mn}^2 + B_{mn}^2}{I_{mn}} V_m V_n \sin \delta_{mn} \tag{3.34}$$

$$\frac{\partial I_{mn}}{\partial \delta_n} = -\frac{G_{mn}^2 + B_{mn}^2}{I_{mn}} V_m V_n \sin \delta_{mn} \tag{3.35}$$

$$\frac{\partial I_{mn}}{\partial V_m} = \frac{G_{mn}^2 + B_{mn}^2}{I_{mn}} (V_m - V_n \cos \delta_{mn}) \tag{3.36}$$

$$\frac{\partial I_{mn}}{\partial V_n} = \frac{G_{mn}^2 + B_{mn}^2}{I_{mn}} (V_n - V_m \cos \delta_{mn}) \tag{3.37}$$

3.1.8. GAIN MATRIX AND NUMERICAL PROPERTIES

With the help of Jacobian measurement matrix **H** and the measurement error covariance matrix **R**, the gain matrix **G** is formed as shown in equation (3.38). The gain matrix is symmetric and sparse as compared to the Jacobian measurement matrix. It is positive definite for observable networks [37].

$$G\left(x^k\right) = H^T R^{-1} H \tag{3.38}$$

3.2. ALGORITHM MODELLING

The algorithm of WLS Estimation based on maximum likelihood is explained.

3.2.1. MAXIMUM LIKELIHOOD ESTIMATION

The measurement vector is stochastic because of the noise present. The state vector is not accurately determined and hence a flat start is generally taken. A conditional probability density function $\mathbf{f(z \mid x)}$ is considered for unknown state vector $\mathbf{x}$. To obtain $\mathbf{x}$ from $\mathbf{f}$, maximum likelihood criterion is followed as stated by F.L.Lewis[39]:

The maximum-likelihood estimate $\hat{x}$ for a given measurement z is the value of x which maximizes $\boldsymbol{f(z \mid x)}$, the likelihood that x resulted in the observed z.

The log of likelihood function $\mathbf{f(z \mid x)}$ is defined to make solving easier. Log is always monotonically increasing function which implies that the maximisation of $\mathbf{ln(f(z \mid x))}$ is equivalent to maximisation of $\mathbf{f(z \mid x)}$. The problem is solved here by minimising as shown in equation (3.39).

$$\underset{\mathbf{x}}{\text{Minimise}} : -\ln(f(\mathbf{z} \mid \mathbf{x})) \tag{3.39}$$

$\mathbf{z}$ is considered to be normally distributed as shown in equation (3.40):

$$f(\mathbf{z} \mid \mathbf{x}) = \frac{1}{\sqrt{(2\pi)^m \det R}} e^{-\frac{1}{2}(\mathbf{z}-\mathbf{h}(\mathbf{x}))^T R^{-1}(\mathbf{z}-\mathbf{h}(\mathbf{x}))} \tag{3.40}$$

The minimisation problem of equation (3.39) can be written as follows:

$$\underset{\mathbf{x}}{\text{Minimise}} : \quad J = \frac{1}{2}(\mathbf{z}-\mathbf{h}(\mathbf{x}))^T R^{-1}(\mathbf{z}-\mathbf{h}(\mathbf{x})) \tag{3.41}$$

The solution to this problem is known as Weighted Least Squares Estimation of $\mathbf{x}$. The solution is reached by using Gauss-Newton method shown below.

3.2.2. GAUSS-NEWTON METHOD

In order to find $\hat{x}$, approximations to first and second derivatives of $\mathbf{J}$ are applied. The following condition has to be satisfied at first derivative shown in equation (3.42).

$$\nabla_x J(\mathbf{x}) = -H^T(\mathbf{x}) R^{-1}[\mathbf{z}-\mathbf{h}(\mathbf{x})] = 0 \quad \left(H(x) = \frac{dh(x)}{dx}\right) \tag{3.42}$$

On expanding the equation (3.42) around state vector $\hat{x}$ with Taylor's series expansion:

$$\nabla_x J(\mathbf{x}) = \nabla_x J\left(\mathbf{x}_p\right) + \nabla_x^2 J\left(\mathbf{x}_p\right)\left(\mathbf{x}-\mathbf{x}_p\right) + \ldots = 0 \tag{3.43}$$

Substituting equation (3.42) in equation (3.43) to find the second order derivative and neglecting higher order terms:

$$\nabla_x^2 \mathbf{J}(\mathbf{x}_p) = \mathbf{H}^T(\mathbf{x}_p)\mathbf{R}^{-1}\mathbf{H}(\mathbf{x}_p) \tag{3.44}$$

Substituting equations (3.42) and (3.44) in 3.43, the x_p iterates (where $\boldsymbol{p}$ is the iteration count) can be calculated [40]:

$$\mathbf{x}_{p+1} = \mathbf{x}_p + \left[H^T(\mathbf{x}_p)R^{-1}H(\mathbf{x}_p)\right]^{-1} H^T(\mathbf{x}_p)R^{-1}\left[\mathbf{z} - \mathbf{h}(\mathbf{x}_p)\right] \tag{3.45}$$

This can be simplified to equation (3.46) using equation (3.38):

$$\Delta\mathbf{x}_{p+1} = \mathbf{G}^{-1}(\mathbf{x}_p)\mathbf{H}^T(\mathbf{x}_p)\mathbf{R}^{-1}\left[\mathbf{z} - \mathbf{h}(\mathbf{x}_p)\right] \tag{3.46}$$

where

$$\Delta\mathbf{x}_{p+1} = \mathbf{x}_{p+1} - \mathbf{x}_p \tag{3.47}$$

3.3. OVERVIEW OF THE ALGORITHM

The non-linear WLS algorithm involves solving of equation (3.46) iteratively. The initial system states are assumed; generally a flat start with all voltage magnitudes as 1 p.u. and bus angles as 0 degrees. The iterative algorithm steps are shown below and in figure 3.4 as a flowchart.

1. Initialise the state vector, set the iteration index as p=1 and set a tolerance value.
2. Calculate the measurement functions **h(x)** and also the residual **r** by subtracting the given measurements with the computed ones from measurement functions.
3. Calculate the Jacobian measurement matrix **J**.
4. Calculate the Gain matrix **G**.
5. Check if absolute value of $\Delta\mathbf{x}_{p+1}$ is less than the tolerance set.
6. If yes, **STOP**
   else Update $\mathbf{x_{p+1}}$ and $p = p + 1$; go to step 2 and repeat the steps.

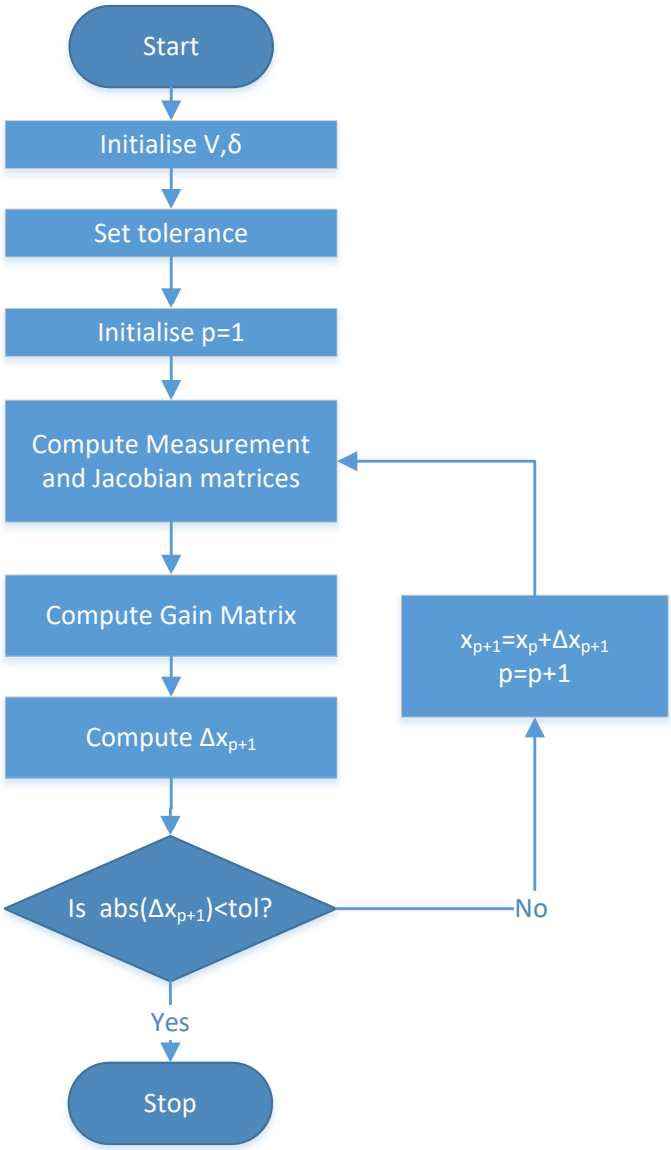

Figure 3.4: Flow Chart of WLS Algorithm

3.4. OBSERVABILITY OF THE NETWORK

State estimation can be performed under the condition that the system is observable. To ensure this, the rank of Jacobian matrix **J** should be greater than or equal to **n**, the total number of states to be estimated in the state vector matrix. For Gauss-Newton

approach to be applicable, this has to be ensured to allow invertability of the matrix.

3.5. CONDITION NUMBER

Condition number of an invertible square matrix is used to quantify the validity of solution vector obtained [41]. To calculate the condition number, the norm of a matrix has to be defined. The norm is always positive and defined for all types of matrices: square/rectangular or invertible/non-invertible. Norm is denoted by $||A||$ for the matrix shown in equation (3.48).

$$\mathbf{A} = \begin{bmatrix} a_{11} & \cdots & a_{1n} \\ \vdots & \vdots & \vdots \\ a_{m1} & \cdots & a_{mn} \end{bmatrix} \tag{3.48}$$

3.5.1. NORM OF A MATRIX

The norm $||A||$ of a matrix can be calculated in multiple ways but should satisfy these properties as stated in [42], [43].

1. $||A|| \geq 0$ for any matrix.
2. $||A|| = 0$ is equal to zero if and only if the A is a null matrix.
3. $||kA|| = |k|\ ||A||$, for any scalar k.
4. $||A + B|| \leq ||A|| + ||B||$
5. $||AB|| \leq ||A||\ ||B||$

Based on these, few of the definitions of calculating it are shown in table 3.1 which are used most extensively. The condition number is then defined as shown in equation (3.49). The notation is adjusted as $||A||_\infty$ or $||A||_1$ or $||A||_E$ depending on the type of norm used.

$$\kappa(A) = ||A||\ ||A^{-1}|| \tag{3.49}$$

This section has been largely summarized from [42].

Table 3.1: Methods to compute norm of matrix [42], [43]

Type	Definition	Representation
1-Norm	Maximum of the sum of absolute values down each column.	$\|\|A\|\|_1 = \max_{1 \le j \le n} \left(\sum_{i=1}^{m} \|a_{ij}\| \right)$
Infinity norm	Maximum of the sum of absolute values across each row.	$\|\|A\|\|_\infty = \max_{1 \le i \le m} \left(\sum_{j=1}^{n} \|a_{ij}\| \right)$
Euclidean norm	Square root of sum of squares of all the elements in the matrix.	$\|\|A\|\|_E = \sqrt{\sum_{i=1}^{m} \sum_{j=1}^{n} (a_{ij})^2}$

Based on the value of $\kappa(\mathbf{A})$ for all the norms, the matrix is classified as well or ill conditioned for all the norms.

- **Well-Conditioned:** A system of equations is well conditioned if a small change in coefficient matrix results in a small change in the solution vector. The condition number is low.
- **Ill-conditioned:** A system of equations is ill conditioned if a small change in coefficient matrix results in a large change in the solution vector. The condition number is high.

Numerically if $\kappa(\mathbf{A})$ is much larger than 1, the matrix is said to be ill-conditioned. The condition number of the matrix should therefore be as low as possible to ensure that the results obtained are accurate. This has been considered throughout the project and ensured that the condition number is reasonable to trust the results obtained.

4

Dutch MV grids and Study Systems Setup

In this chapter, a basic overview of the Dutch distribution Network is provided and the considered system setups are explained in detail.

4.1. Dutch Grids Description

The Dutch grid essentially can be divided into three categories, namely [44]

1. **National Grids:** Consists of 220kV and 380kV with overhead lines.
2. **Regional Grids:** Consists of voltage levels between 220kV and 25kV including overhead lines and cables.
3. **Local Grids:** Have cables with voltage levels below 25kV.

These local and regional grids constitute the so called Distribution system which contains the voltage levels below 110 kV and are operated by regional network operators like Alliander, Enexis, Stedin etc. The voltage levels starting from 110 kV and above are of the transmission level and handled by TenneT. Few DSOs do manage a part of 110 kV/150 kV network, but is negligible [45]. Most of the MV Distribution networks in the Netherlands are rated at 10 kV. These MV networks are mostly radially operated regardless of the structure. The LV networks are connected with cables in radial structure. Most of the MV networks in the Netherlands consist of underground cables. These networks transport electricity from the primary substations to multiple MV nodes in the network.

4.2. NETWORK DATA

The National Grid of the Dutch Electricity Network is managed by **TenneT** that connects most of the regional grids and power plants. The network length data in addition to the type (underground cables or overhead lines) for different voltage levels of the network in Netherlands is shown in table 4.1 [45]. Since most of the MV and LV networks are underground cables, they are fairly independent to changes in weather. Due to the extensive and sophisticated protection system coupled with network structure, the Dutch energy grid is one of the most reliable in the world.

Table 4.1: Overview of Networks in Netherlands [45]

Voltage level(kV)	Overhead lines (km)	Underground cables (km)
380 (Transmission,HV)	2137	28
220 (Transmission,HV)	699	9
150 (Transmission,HV)	2893	885
110 (Transmission,HV)	1859	398
50 (Distribution,MV)	270	2481
25-30 (Distribution,MV)	0	1926
20 (Distribution,MV)	0	1947
6-12.5 (Distribution,MV)	0	100071
3-5 (Distribution,MV)	0	1720
0.4 (Distribution,LV)	180	220449

This data comprises of network information from various network operators like TenneT TSO, Enduris, Liander, Enexis BV, Stedin BV, NV Rendo, Westland Infra, Endinet and Cogas Infra & Beheer BV. The total network length is around 310,000 kms.

4.3. STRUCTURE OF MV DISTRIBUTION NETWORKS

Most of the MV distribution networks have a voltage level of 10kV. Typically, these networks are ring or mesh shaped and are radially operated [46]. At the substation level, a transformer is placed to lower the voltage to required medium level from a higher voltage level. Essentially, there are three types of networks but all of them are radially operated and are identical when considered by the state estimator. There are networks which do operate at a higher voltage levels (20-50 kV) and are often operated in a meshed way with a non-radial topology but they haven't been considered here in this thesis.

4.3.1. RADIAL STRUCTURE

This is the simplest structure of all. This is put in place in areas of low concentration of customers. Not extensively used in the Netherlands because of a lack in fault contingency. The network structure is shown in figure 4.1.

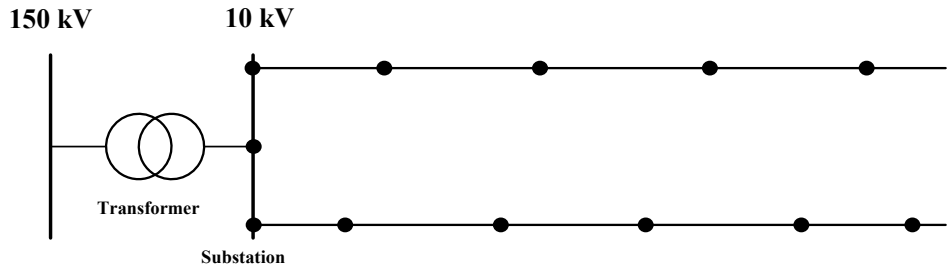

Figure 4.1: Radial Network

4.3.2. RING SHAPED STRUCTURE

Most of the networks are constructed in this way such that the ends meet forming an annular structure. In the ring structure, at some place a network opening (normal open point) is provided which can be used for network reconfiguration. First, the faulted section of the network is isolated, then the normal open point circuit breaker is closed. This helps to minimise the number of disconnected clients in case of a disturbance. The network structure is shown in figure 4.2.

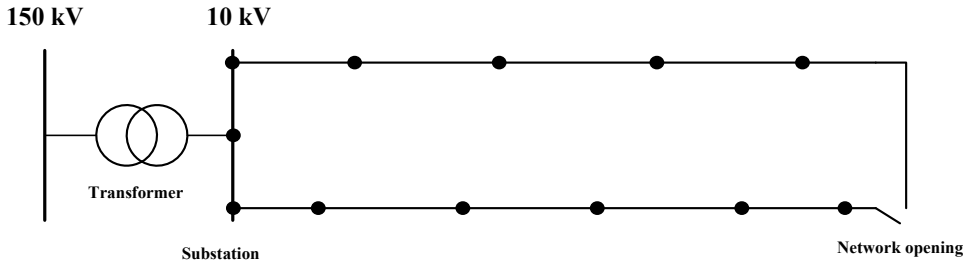

Figure 4.2: Ring Network

4.3.3. MESHED STRUCTURE

In the ring structure, there is one point of fault reserve (the network opening). This structure can be further expanded such that multiple lines or strands meet at points where different grid openings are provided. One of the main advantages of this type of a structure is that there is more scope of power distribution all across the network.

This structure is predominant in densely occupied cities or industrial areas. The network structure is shown in figure 4.3.

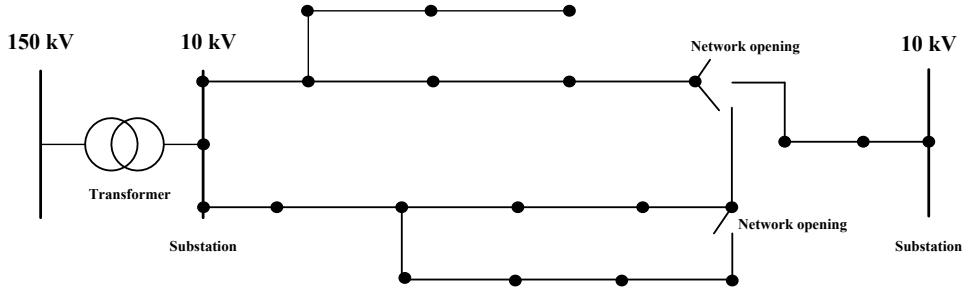

Figure 4.3: Meshed Network

4.4. MV MONITORING

SCADA monitoring is predominant in MV networks from a long time now. SCADA essentially compiles and sends near real time information about the grid to a central data processing hub. The main components of SCADA are [47] :

- **Field Instrumentation(Meters):** These detect the changes in the grid parameters like voltage, current and so on. This data is then sent to the Remote Terminal Units (RTUs) and Programmable Logic Controllers (PLCs) for further processing.
- **Field Controllers(RTUs/PLCs):** The data collected from the field instruments is processed by these controllers to be displayed and analyzed by the Human Machine Interface (HMI). RTUs rely on microcontrollers and microprocessors for data conversion suitable to central processing hub. Since the PLCs operate locally, direct interface with the meters and sensors to the data hub is possible.
- **Human Machine Interface(HMI):** HMI are the units where humans are allowed to oversee the data acquisition process of SCADA system. It acts as a central processor to SCADA and allows users to view the information at one place.
- **Network connectivity/Communication:** For SCADA to monitor information effectively, the connectivity in the network has to be foolproof. Many networking and communication protocols are put in place for this very reason.
- **Database:** Post analyzing the gathered data, the information has to be stored securely. This is done in secured cloud servers in detailed manner to make it easier for later reference.

4.5. VISION NETWORK ANALYSIS COMPONENT DESCRIPTION

As part of this thesis, Vision NA is used to build the networks that are studied as a single line diagram. A single line diagram essentially constitutes of a very simplified representation of a balanced three phase system. In the networks constructed, there are both medium voltage and low voltage loads are present. It is important to note that the loads considered are aggregate of many households and not a single household in particular. Each of the load includes various type of consumers with many possibilities of load profiles and power consumption.

The various components used to mimic the real life equipments used in a power grid as part of Vision NA for this thesis are shown in figure 4.4 and explained in detail.

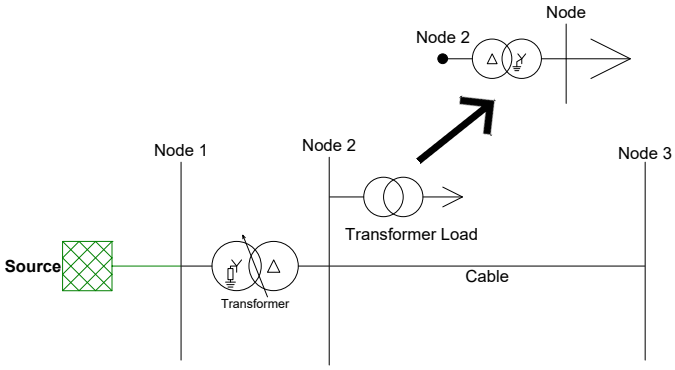

Figure 4.4: Various components used in Vision Network analysis

4.5.1. NODES

The nodes are the bus stations that are connected through branches which are the cables as well as the transformers. The nominal operating voltage for the first network is set at 10.6 kV and 13 kV for the second one which is the medium voltage level and 400 V for the LV level.

4.5.2. CABLE

The cables in the network represent a three phase connection between two nodes. A single cable in a network is made of different cable types which change along the length of the line. Apart from this, the ampacity factor as well as the nominal current for each of the cable type is specified. These are shown in figure 4.5. The modelling of cable is done using π-model as explained in figure 3.1.

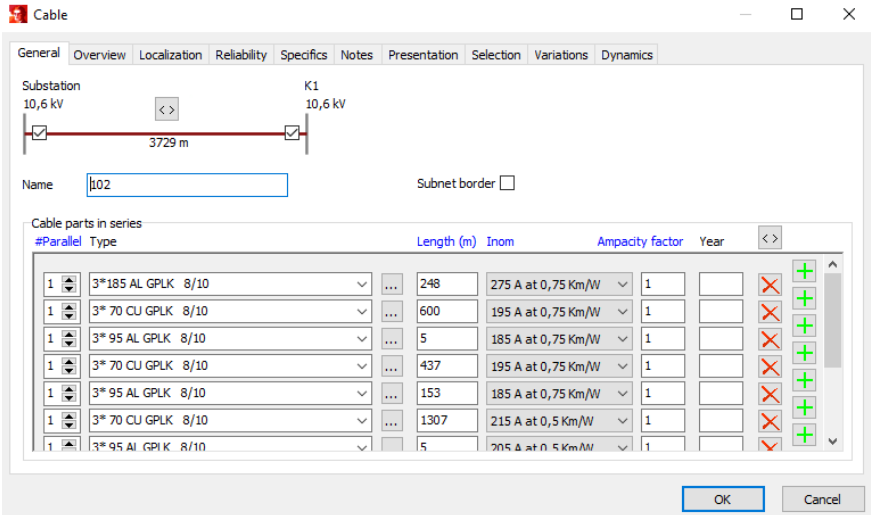

Figure 4.5: Cable parameters in Vision Network Analysis

4.5.3. Transformers and Transformer Loads

The transformers are used to connect two subsystems with different voltage levels. A vivid element used in Vision NA software is the transformer load. All the DSOs in the Netherlands use this element as part of their design networks. In distribution networks, the transformers are used mainly to step down the voltage from a transmission level all the way to residential level.

In Vision NA, an element which is the combination of a transformer and load is present as shown in figure 4.4. The load is connected to the secondary of the transformer. This element is used in the modelling of the network shown in figure 4.6 & figure 4.7. To visualise better, the transformer and load are represented separately. In the two networks considered above (figure 4.6 & figure 4.7), the transformer loads have alrady been split for more clarity to be shown in the schematics.

4.5.4. Source/Grid

The source is considered as the swing bus which is used as the reference for all the calculations. In Vision NA, one source is present in a network (generally connected to the substation). The main role of the source is to maintain balance in the network by providing the mismatch between the generation and loads with power losses in the network considered.

4.6. STUDY SYSTEMS CONSIDERED

The first network represents a typical network and the load measurements are generated synthetically using the ALPG tool explained in chapter 5. In the second network, the measuring devices measurements are available for few of the loads. It is assumed that the grid topology remains constant and free from faults and failure in components. All the further analysis done in upcoming chapters is performed on these two networks. The information corresponding to various components present in the two networks is found in table 4.2.

Table 4.2: Components in the networks considered

Element	Network 1	Network 2
Nodes	65	28
Cables	35	11
Source	1	1
Transformers	32	16
Loads	32	16

The detailed information of the two networks is included in Appendix B and Appendix C.

4.6.1. NETWORK 1

An anonymized 65 bus typical Dutch MV distribution network is considered as one of the test cases. The MV grid is rated at 10.6 kV and has a primary substation rated at 10.6 kV which is taken as reference or the slack node for all the analysis. The schematic of the grid is shown in figure 4.6.

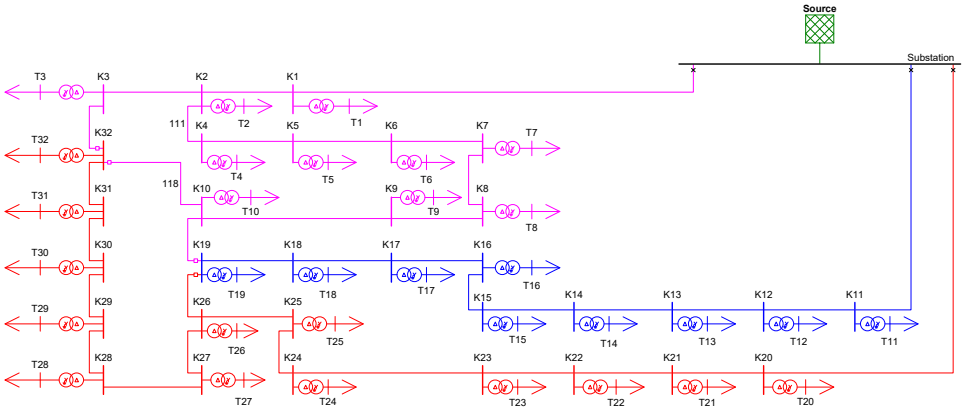

Figure 4.6: Test Network built in Vision

The network has 65 nodes, 32 of which are connected to LV loads representing multiple households. The different colors represent separate feeders which can be reconfigured if and when needed using the network openings provided. Step down 10.6/0.4 kV transformers with different MVA ratings are used. The transformers are rated in accordance to the size of the LV network varying from 0.25 MVA to 0.63 MVA. When generating the load scenarios, it is made sure that for the actual case, the LV network nodes are loaded more than 30% of the transformer rating at that end. For each run of the state estimation algorithm, loads are generated using the ALPG tool.

4.6.2. NETWORK 2

An anonymized and downsized MV distribution network owned by Stedin B.V., a Dutch DSO, is taken. The grid contains a 50/13 kV transformer in the primary substation which is considered as the slack node. Step down transformers corresponding to 13/0.4 kV voltage level are used along with 50/13 kV transformer at the primary substation. The network has been modelled in Vision NA as shown in figure 4.7.

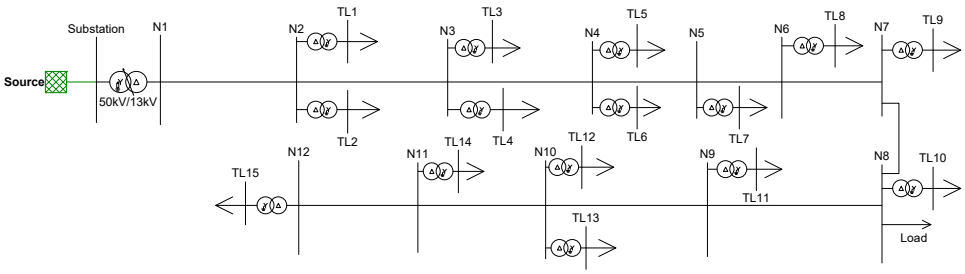

Figure 4.7: Test Network of Stedin B.V built in Vision

The network comprises of 28 nodes with 15 of them connected to household loads. The measuring devices data for few of these loads are available and for the other loads, a general overview of the loading profile over the entire year is available which can be used as a basis for generating pseudo-measurements.

4.7. EXPORTING TO MATPOWER

The networks implemented in Vision NA are exported to MATLAB as Matpower files for further testing. A tool developed for this exact purpose is used. The user interface of this tool is shown in Appendix A.

The active and reactive powers of the components is determined which form the columns P_d, Q_d, G_s and B_s in the matpower file which translate to active power, reactive power, shunt conductance and shunt susceptance demands respectively. G_s

and B_s are calculated at 1 p.u. The active and reactive powers are exported directly as MW & MVar. The loads at the buses are summed up during this process. The sign convention is positive for loads and negative for generation. The source/grid is considered as synchronous generator during the conversion. The bus types are determined as follows

- **Slack bus:** The bus connected to the source or the external grid.
- **PV bus:** The bus connected not to a source but to a synchronous generator in voltage-control mode. These buses are not present in the considered study systems.
- **PQ bus:** The bus which does not fall in the other two categories.

The cables connecting nodes are considered as branches and are exported to Matpower in p.u. format. The cable structure is shown in the figure 3.1 with no shunt conductances. The equivalent resistance is $\boldsymbol{R}$, reactance $\boldsymbol{X}$ and shunt capacitance $\boldsymbol{C}$. These are converted to per unit form as shown in equation (4.1), equation (4.2) and equation (4.3) [38].

$$r = \frac{R}{Z_{base}} \tag{4.1}$$

$$x = \frac{X}{Z_{base}} \tag{4.2}$$

$$b = 2\pi f C Z_{base} \tag{4.3}$$

where the base impedance is determined from the nominal voltage of the buses and the base apparent power as shown in equation (4.4) [38]. The nominal frequency is taken as 50 Hz and the base apparent power is considered as 10 MVA.

$$Z_{base} = \frac{V_{base}^2}{S_{base}} \tag{4.4}$$

Another parameter that needs to be converted is the transformer with a tap that can affect the transformer modelling. This modelling is explained in Chapter 3. Depending on the position of the tap changer, the tap parameter $\boldsymbol{a}$ can be calculated as shown in equation (4.5) and equation (4.6) [38].

$$a = \frac{V_{nom}^n}{V_{nom}^m} . \frac{V_{nom}^{pr} + \Delta V \times pos}{V_{nom}^{sec}} \tag{4.5}$$

$$a = \frac{V_{nom}^{n}}{V_{nom}^{m}} . \frac{V_{nom}^{pr}}{V_{nom}^{sec} + \Delta V \times pos} \tag{4.6}$$

where, V_{nom}^{m} and V_{nom}^{n} are the nominal voltages of primary and secondary buses. V_{nom}^{pr} and V_{nom}^{sec} are the primary and secondary nominal voltages of the transformer windings. ***pos*** is the position of tap changer. Magnetising currents and no-load losses of transformer shunt branches are neglected.

5

Measurement Modelling

This chapter helps in answering the way measurements are used for the state estimation algorithm. Two ways of modelling the measurements for the networks considered in this thesis are explained in detail:

- The synthetic modelling of measurements and their corresponding variances are explained which are used for the network in figure 4.6.
- Using measuring devices data and historical load profile data over the entire year for the network in figure 4.7.

The synthetic modelling of data is to check the viability of the algorithm on a real network with respect to few of the statistical measures. It also gives a lot of freedom to vary the inputs and observe how the algorithm responds. With the measuring devices data, it is further analysed how a change in input variables can affect the estimated results. The algorithm's response to redundancy and type of measurement being used as an input can be recognised which can prove to be quite instrumental in implementing the state estimator for real world applications.

5.1. Synthetically modelled data

Various Demand Side Management (DSM) techniques have been developed over the past few years which can accurately model synthetic load profiles according to the grid requirements. One such load modelling technique proposed in [7] is used in this thesis.

The load data at each of the nodes is generated artificially. For this, multiple load profiles are generated using the ALPG tool developed by Dr.ir. G. Hoogsteen [7],

[8]. The process is shown as a flowchart in figure 5.1 and explained in detail in this section.

5.1.1. LOAD PROFILE GENERATION

Each of the node/bus in the considered network is managed by the corresponding DSO. Few of these are connected to industrial loads and the remaining are assumed to be connected to neighbourhood of households. At each of the MV node that is connected to a LV network, load profiles are generated. The loads connected to this LV network are assumed to be residential households. The number of households at each of the nodes is specified (typically a LV network consists of 70-80 households). The average solar irradiation data is available for the Netherlands [48]. The individual load profiles are generated for the specified number of households using ALPG and the summation of these profiles gives the total load of the LV network. Active and reactive power profiles are generated by implementing a bottom up approach using the ALPG tool [8]. The steps below are followed by the algorithm to generate the residential load profiles:

- The number of households in the neighbourhood to be simulated is taken as input (most of the neighbourhoods have 70-80 households for the network considered).
- The availability and penetration percentage of Photo-Voltaic Panels and other flexible loads are to be specified as shown in table 5.2.
- The occupancy profile of households is simulated using behaviour of each individual which is based on the table 5.1.
- Each device is given a power factor and accordingly reactive power profiles are generated.

Table 5.1: Household Configurations [8]

Name	Annual consumption(kWh)	Persons (Adults)
Single Worker	1610 – 2410	1(1)
Dual Worker	2660 – 4060	2(2)
Family Dual Worker	3460 – 7060	3 – 6(2)
Family Single Worker	3460 – 7060	3 – 6(2)
Family Single Parent	2600 – 6200	2 – 5(1)
Dual Retired	2660 – 4060	2(2)
Single Retired	1610 – 2410	1(1)

Seven household configurations have been predefined as shown in table 5.1 and

for each of the nodes, combinations of these seven households have been simulated to make up the entire neighbourhood.

5.1.2. LOAD SCENARIOS

The load scenarios are generated at each of the MV nodes which are connected to a LV network by creating load profiles using ALPG as explained in section 5.1.1. Each of the MV networks comprises certain number of households connected through a LV network. The ALPG algorithm generates active and reactive power profiles of each households for every minute of the day. The algorithm is run multiple times to generate different profiles at each of the LV network. In order to make calculation easier, at each of the LV Network, the profiles are simulated for the seven households in table 5.1.

Table 5.2: Scenarios for load profile generation

Parameter	Scenarios
PV penetration (%)	25 – 75
EV penetration (%)	20 – 60
Households	Variable

The scenarios shown in table 5.2 are considered at different nodes of the network. The household size is set in accordance to the size of the neighbourhood which in most of the cases corresponds to about 70-80 households in the network considered.

APPLYING NORMAL DISTRIBUTION FITTING

Multiple load profiles as explained in section 5.1.1 are generated for each of the LV network node and are used to apply a normal distribution fitting which gives a normal distribution function for each minute of the day. An equivalent load profile for a set of LV loads which is connected to the secondary side of MV/LV transformer. Using these distribution functions, load scenarios are generated. The procedure is described in detail:

- At each of the MV node, multiple load profiles for active and reactive powers are generated and stored in matrices **AP** and **RP**. Assuming $\boldsymbol{M}$ number of profiles are generated for a node $\boldsymbol{n}$ of the total nodes $\boldsymbol{N}$ for every minute of the entire day. The matrices look as shown in equation (5.1) and equation (5.2) for one of the minutes of the day $\boldsymbol{t}$ which is repeated for the entire day:

$$\mathbf{AP}^t = \begin{bmatrix} P^t_{11} & \cdots & P^t_{1N} \\ \vdots & \vdots & \vdots \\ P^t_{M1} & \cdots & P^t_{MN} \end{bmatrix} \tag{5.1}$$

$$\mathbf{RP}^t = \begin{bmatrix} Q^t_{11} & \cdots & Q^t_{1N} \\ \vdots & \vdots & \vdots \\ Q^t_{M1} & \cdots & Q^t_{MN} \end{bmatrix} \tag{5.2}$$

where P^t_{ij} is the i^{th} active power profile of the j^{th} node and Q^t_{ij} is the i^{th} reactive power profile of the j^{th} node of the network at the time instance t.

- For each of the i^{th} profile at every minute **t**, a mean and standard deviation is obtained for both the active as well as reactive power profiles and stored as shown in matrices shown in equation (5.3) and equation (5.4) to further create the load scenarios.

$$\mathbf{P_{mean}} = \begin{bmatrix} P^m_{1_1} & \cdots & P^m_{1_t} \\ \vdots & \vdots & \vdots \\ P^m_{N_1} & \cdots & P^m_{N_t} \end{bmatrix} \qquad \mathbf{P_{sd}} = \begin{bmatrix} P^{sd}_{1_1} & \cdots & P^{sd}_{1_t} \\ \vdots & \vdots & \vdots \\ P^{sd}_{N_1} & \cdots & P^{sd}_{N_t} \end{bmatrix} \tag{5.3}$$

$$\mathbf{Q_{mean}} = \begin{bmatrix} Q^m_{1_1} & \cdots & Q^m_{1_t} \\ \vdots & \vdots & \vdots \\ Q^m_{N_1} & \cdots & Q^m_{N_t} \end{bmatrix} \qquad \mathbf{Q_{sd}} = \begin{bmatrix} Q^{sd}_{1_1} & \cdots & Q^{sd}_{1_t} \\ \vdots & \vdots & \vdots \\ Q^{sd}_{N_1} & \cdots & Q^{sd}_{N_t} \end{bmatrix} \tag{5.4}$$

where P_{mean} comprises of the mean and P_{sd} comprises the standard deviation of the active power profile distribution. Similarly, Q_{mean} comprises of the mean and Q_{sd} comprises the standard deviation of the reactive power profile distribution.

CREATING LOAD SCENARIOS

The load scenarios are generated by at each of the instant in time (every minute) for all the nodes from the normal distribution. These form matrices $\mathbf{Load_{Pi}}$ and $\mathbf{Load_{Qi}}$ shown in equation (5.5) for the i^{th} scenario with load profiles l_{Pi_j} and l_{Qi_j} of the j^{th} connected node.

$$\mathbf{Load_{Pi}} = \begin{bmatrix} l_{Pi_1} \\ \vdots \\ l_{Pi_N} \end{bmatrix} \qquad \mathbf{Load_{Qi}} = \begin{bmatrix} l_{Qi_1} \\ \vdots \\ l_{Qi_N} \end{bmatrix} \tag{5.5}$$

where l_{Pi_j} and l_{Qi_j} are generated by drawing samples from a Normal Distribution and keeping track of the power factor.

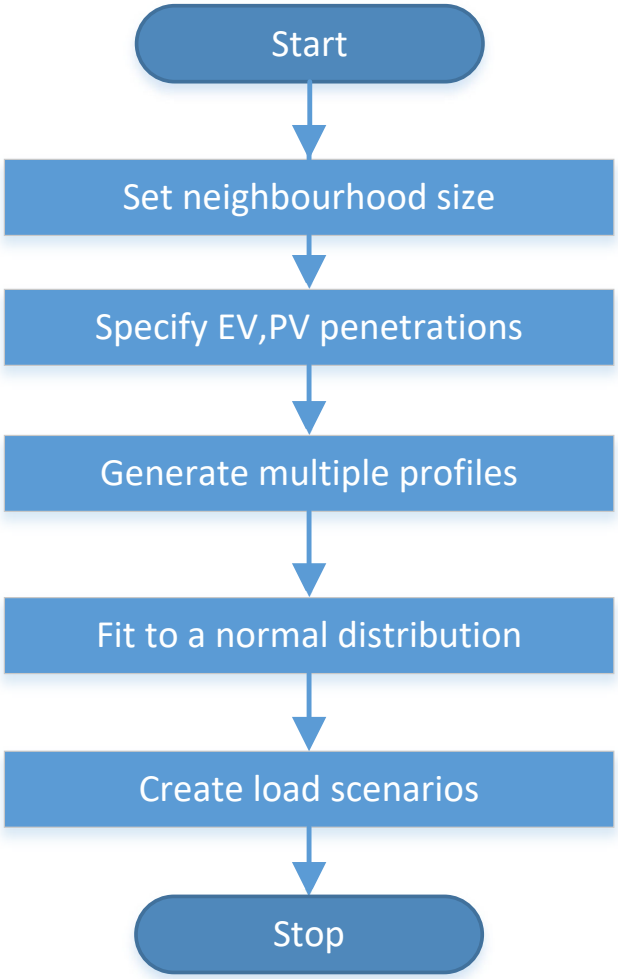

Figure 5.1: Measurement modelling flowchart

5.1.3. CREATING MEASUREMENTS

After the loading scenario is generated, real measurements are created by running the power flow by providing the power injection values as input ($\mathbf{P_{injection}} = -\mathbf{Load_{Pi}}$ and $\mathbf{Q_{injection}} = -\mathbf{Load_{Qi}}$). After the power flow is run, the true measurements of bus voltage magnitudes and angles are obtained at every minute along with the power flows. The true system state is obtained which is represented by $\mathbf{V_{true}}$ and $\boldsymbol{\delta}_{\mathbf{true}}$.

To apply the State Estimation algorithm, variances of the different kinds of measurements also have to be taken into account.

SIMULATED REAL MEASUREMENTS

These are the measurements which are taken from the measuring devices from different points of the grid. In this scenario, these are the measurements generated by using the ALPG and are considered to be quite accurate. The variance of the measured value depends on the sensitivity of the meter used which is assumed to be 10^{-5} [49]. The real measurements are simulated by drawing samples from the distribution fit at various instances.

VIRTUAL MEASUREMENTS

These are the buses with no loads and hence the active and reactive power injection values are zero. The variance for these measurements is very low and is taken as 10^{-7}. A non-zero value is taken so as to prevent the singularity of the error covariance matrix when inverted.

PSEUDO MEASUREMENTS

These comprise of the nodes with missing measurement values which is due to the absence of measurement meters. At these points, the measurements are formulated using the profiles from the ALPG which are based on the general behaviour of the neighbourhood (assumed to be historical load profiles). The variance is equal to the values obtained from the normal distribution function and the injection values are equal to the mean of the distribution function at each instant of time. This is because these are the best possible estimates that are obtained from the load profiles generated. A good and unbiased forecast is assumed here.

5.1.4. DETERMINING TRUE STATES

Newton-Raphson PF is employed taking all the real measurements to find the true system states in order to check the validity of the solution from the state estimator. In this case there are no pseudo-measurements and the power flow is run for each minute of the day. The power flow does converge for all the instances considered.

5.1.5. STATE ESTIMATION ALGORITHM ERROR

The SE Algorithm is implemented for the network model and the obtained system states, the voltage magnitude $\mathbf{V}$ and the bus angle $\boldsymbol{\delta}$ are compared with the true system states. The error percentage is obtained by (for a node i):

$$\text{Error} = \frac{|\mathbf{V_{se_i}} - \mathbf{V_i}|}{|\mathbf{V_i}|} * 100 \tag{5.6}$$

where $\mathbf{V_{se_i}} = \mathbf{V_{mag_i}} \angle \boldsymbol{\delta_i}$ and $\mathbf{V_i} = \mathbf{V_{true_i}} \angle \boldsymbol{\delta_{true_i}}$.

In a similar way, the absolute error is calculated for all the nodes in the network for the entire time period. The mean of all the errors of individual nodes is also calculated.

5.2. MEASUREMENT DEVICES DATA

The network in figure 4.7 has data from the measuring devices and the historical energy consumption data with which an average load profile for the entire year has been estimated. In distribution networks, the measuring devices are placed at few of the transformers and therefore it is possible to get the total power injection at that node. It is to be noted that the values from a meter correspond to the whole neighbourhood and not a single household. It is in fact not possible to get this data from each of the nodes (neighbourhoods) at every instant. This is why, the previously measured values are kept intact to be used to estimate the most probable value from the distribution fit which is again normal [33].

The frequency of measurements of the devices is five minutes apart. This implies that the value obtained is the averaged one for those five minutes. Ten of the sixteen nodes which have loads have measuring devices installed. The other six nodes with loads have load power profiles that have been generated for the whole year using a bottom up approach. These load profiles are considered to calculate the variance and the mean value of power injections for the required time frame. Similar to how the profiles have been sampled in the synthetic data modelling case, the load profiles are sampled here too to get the simulated power injection values (used as pseudo-measurements). Again, measurements play an important role to check the validity of the algorithm.

5.2.1. MEASUREMENTS

Similar to the synthetic measurements modelling case, the type of measurements are divided into three categories.

SIMULATED REAL MEASUREMENTS

These are the measurements that are considered from the measuring devices readings at few of the nodes near the transformers. These can be relied upon and hence has a small variance associated which is taken as 10^{-5} [49].

VIRTUAL MEASUREMENTS

Similar to the earlier case, these are the buses with no loads and a small variance of the order 10^{-7} is taken into account to not affect the computations.

PSEUDO MEASUREMENTS

These comprise of the nodes with missing measurements and are derived from the load profiles that has been documented by the DSOs from historical load profile data. The active power injection profiles are used to compute the reactive power injection profiles using the power factor which is specified for the loads that are considered.

5.2.2. VALIDITY OF THE ALGORITHM

The true states of few of the nodes are available from the measuring devices data which are used as the basis for comparision of the estimated values from the state estimation.

6

Results and Discussion

This chapter comprises of the various analysis done on the two selected test networks and how the selected WLS algorithm fits into the larger picture for state estimation in distribution networks.

6.1. Statistical test of the algorithm

To check if the algorithm is indeed effective for distribution network applications, a statistical test is done. The two measures used are bias and consistency which are described below and summarized from [22].

6.1.1. Bias

Statistical bias is said to exist if the estimated parameter is not systematically different. If the expected error is zero, then the estimator is said to be unbiased. Equation (6.1) shows the mathematical equivalent of an unbiased estimator where $\boldsymbol{x}_t$ is the true state vector and $\hat{\boldsymbol{x}}$ is the estimated state vector :

$$E\left[(\boldsymbol{x}_t - \hat{\boldsymbol{x}})\right] = \mathbf{0} \tag{6.1}$$

6.1.2. Consistency

In statistics, an algorithm or a procedure which adheres to certain confidence intervals upon tests with a hypothesis is sought after. An estimator is consistent if the estimates converge in probability to the value the estimator is designed to estimate. One of the measures for consistency is the normalised state error squared variable shown in equation (6.2) where $\hat{\boldsymbol{R}}_{\boldsymbol{x}}$ is the estimated error covariance matrix :

$$\epsilon = (\boldsymbol{x}_t - \hat{\boldsymbol{x}})^{\mathrm{T}} \hat{\boldsymbol{R}}_{\boldsymbol{x}}^{-1} (\boldsymbol{x}_t - \hat{\boldsymbol{x}}) \tag{6.2}$$

To determine the consistency of algorithm, it is important that the algorithm lies in certain confidence intervals which is difficult in the multivariate case here. Based on the χ^2-statistics, the limits can be calculated for the multivariate case which is what the result from the estimation algorithm follows. This is theoretically proved based on the Lemma which is taken from [50] stated as follows.

Lemma: If an n-component vector v is distributed according to $\mathcal{N}(0, T)$ (non-singular), then $v^T T^{-1} v$ is distributed according to the χ^2 distribution with n degrees of freedom.

$E\left[(\boldsymbol{x}_t - \hat{\boldsymbol{x}})(\hat{\boldsymbol{x}} - \boldsymbol{x}_t)^T\right]$ is the covariance matrix of estimated errors when the measurement errors are normally distributed [39]. This coupled with the *Lemma* mentioned implies that the normalised mean squared error shown in equation (6.2) should follow a χ^2-distribution for n degrees of freedom (the number of states).

ϵ should lie within a certain interval that is obtained from χ^2-table [51] for chosen confidence level (α) which is generally taken as 95%. The lower and upper bounds for this confidence levels can be arrived at by $\chi^2_n(\frac{(1-\alpha)}{2})$ and $\chi^2_n(\frac{(1+\alpha)}{2})$ [22], [50]. This is explained more in detail in [6].

6

6.2. CASE STUDY

For the purpose of testing the statistical resourcefulness of the algorithm, Network 1 shown in figure 4.6 is considered. The considered setup has 129 states that correspond to the voltage magnitudes and bus angles. WLS algorithm which is explained in chapter 3 is tested here. Various measurements are used with different levels of redundancy taken into consideration.

- **Case 1:** Voltage at slack bus and active & reactive power injections at all the nodes with loads as real measurements.
- **Case 2:** Voltage at slack bus and active & reactive power injections at 50% of the nodes with loads as real measurements.
- **Case 3:** Voltage at slack bus as the real measurement.

Various scenarios are considered with LHS method used for generating the random samples. The advantage of using LHS is the possibility of breaking down a large distributed function into equal probable intervals which enables the selection of samples from not only the most probable region but the entire distribution. This ensures a sense of variability as compared to other brute force techniques which is merely a random samples in few of the cases. This is done using a function **lhsdesign** in MATLAB which generates the random samples depending on the order of variables and number of samples required.

For this case study, the performance of the algorithm against the statistical measures of bias and consistency is measured before delving into the effectiveness of the algorithm.

Figure 6.1 shows the error plot with the number of simulations for the case with 100% pseudo-measurements (worst-case scenario). The error is found by comparing the estimated values from state estimation algorithm with the computed values from the Newton Raphson PF. To ensure that the technique is a good fit, it is important that the error bias has a mean of zero as mentioned previously. It is observed that these estimation errors for the 129 states are slightly indistinguishable due to the overlaps in the figure. Nevertheless, it is seen that the error varies about zero mean and hence the algorithm is unbiased (almost all of the values lie in range of ± 0.05 from zero). It is observed that a similar pattern is found in the rest of the cases too. Hence the algorithm does satisfy this statistical measure.

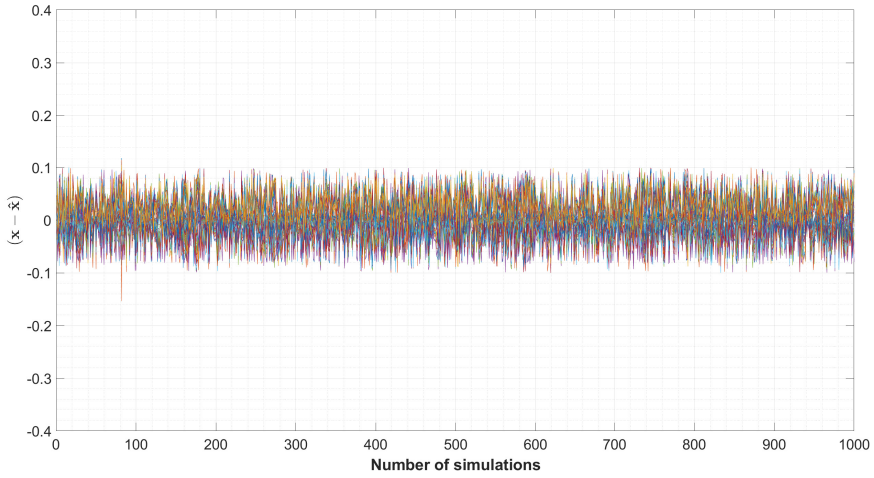

Figure 6.1: Error plot for 100% pseudo-measurement case

Figure 6.2 shows the normalised state error squared variable plotted against 1000 runs of simulations from scenarios created with the help of LHS and it is seen that the algorithm is consistent considering it lies within the bounds defined by the χ^2-table for 129 states at 95% confidence level. The lower and upper bounds are determined from this table to be 99.453 and 162.331. The three cases are considered to assess the consistency of the algorithm and the limits are adhered to throughout. As expected, with decrease in real measurements, the quality of the estimates decreases but the confidence bounds are satisfied in all the three cases. The other interesting observation is that the normalised state error squared variable varies about 129, which is the number of states in the considered system. This is another characteristic of the χ^2 statistics where the point of convergence for consistent algorithms is the number of degrees of freedom of the problem. This shows that the WLS algorithm is consistent.

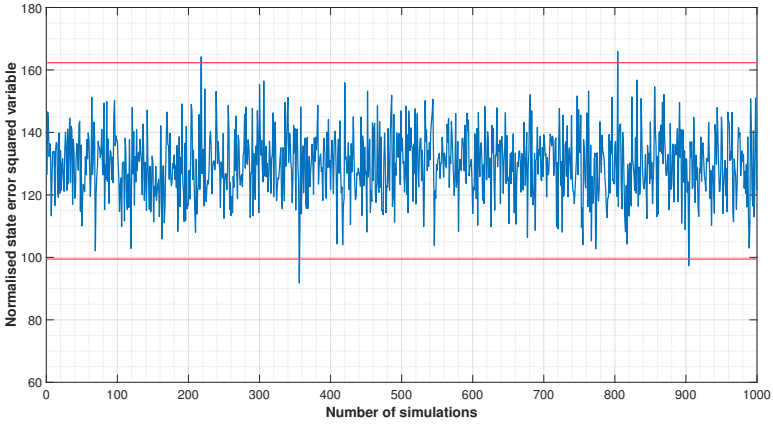

(a) 0% Pseudo-measurements

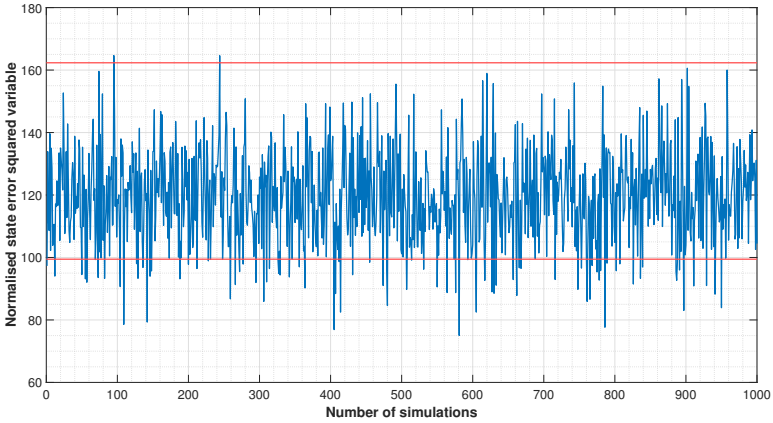

(b) 50% Pseudo-measurements

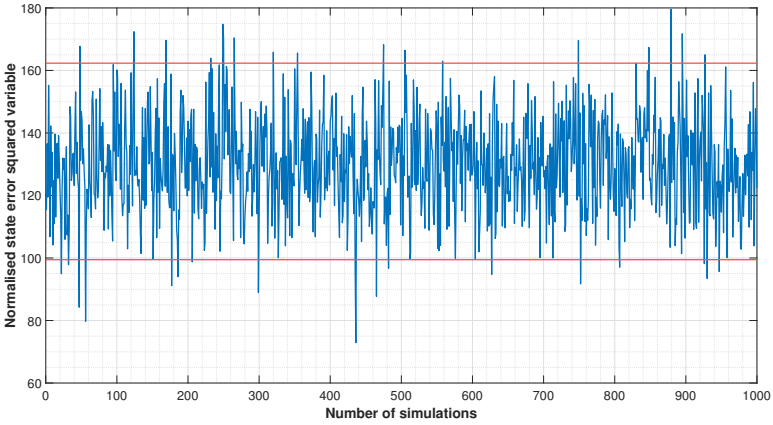

(c) 100% Pseudo-measurements

Figure 6.2: Consistency plots

Since the state variables are assumed to be independent of each other which is not always the case, a few anomalies or a larger noise is seen in the plots. These two tests therefore prove that WLS algorithm is suitable to be used for state estimation in distribution networks. Two other algorithms have been tested in [22] along with WLS and it is concluded that WLS algorithm is the best choice available for this purpose of state estimation in distribution networks.

The algorithm suitable for the purpose of this project has been now narrowed down and the two networks described in section 4.6 are used as study cases to test the WLS algorithm.

6.3. NETWORK 1 WITH SYNTHETICALLY MODELLED DATA

The Network 1 in figure 4.6 is taken as the first test case. Depending on the parameters and the rating of transformers, load scenarios are generated as explained in section 5.1. The load profiles are generated with a time resolution of one minute which implies that the WLS algorithm is run for each minute of the day. Three different cases are considered here with the variation in availability (0%, 50% and 100%) of real measurement data. The state variables and power flows for these cases have been analysed along with the absolute error in determining them.

6.3.1. ABSOLUTE MEAN ERROR

The obtained values from the state estimation algorithm are compared with the ones from Newton Raphson PF to find the absolute mean errors at each of the buses.

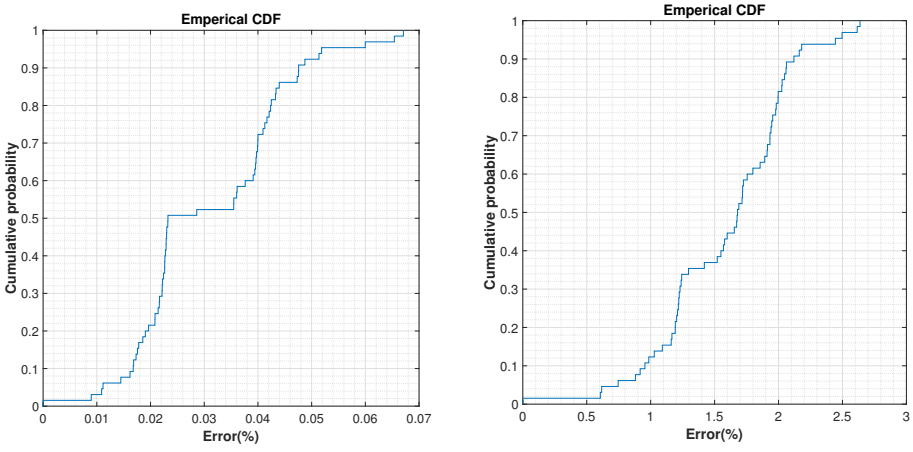

(a) 0% Pseudo-measurements

(b) 100% Pseudo-measurements

Figure 6.3: Mean Error probability of the states in the system

The mean error probability of all the 65 nodes for the 1440 instances are plotted in figure 6.3 for 0% and 100% pseudo-measurements as input to the SE algorithm. From the plots, it can be observed that for the 0% pseudo-measurement case, the state estimation values are very close to the values obtained from power flow which is expected. An increase in injection of pseudo data naturally increases the error in the final states being calculated. It can be concluded that with increased percentage of injection of pseudo data, the emperical cumulative distribution plot tends to move away from the y-axis which implies that there is an increase in the mean absolute error.

6.3.2. EFFECT ON VOLTAGE DUE TO PSEUDO-MEASUREMENTS

To probe in more detail, one of the buses (Bus 2) is singled out to compare the voltage.

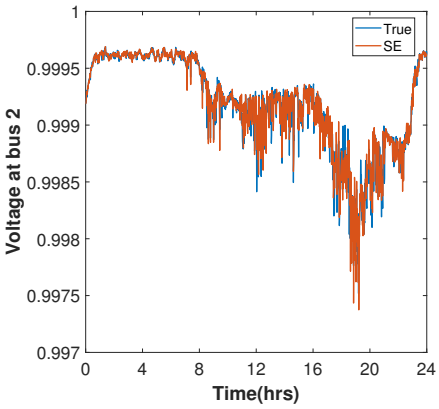

(a) 0% Pseudo-measurements

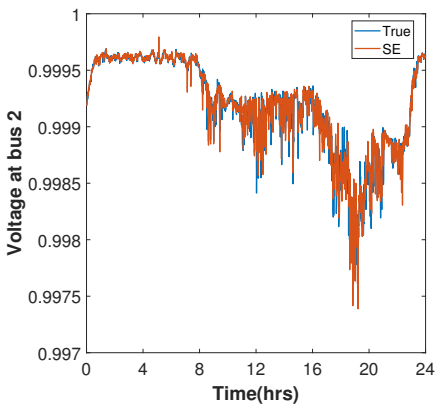

(b) 50% Pseudo-measurements

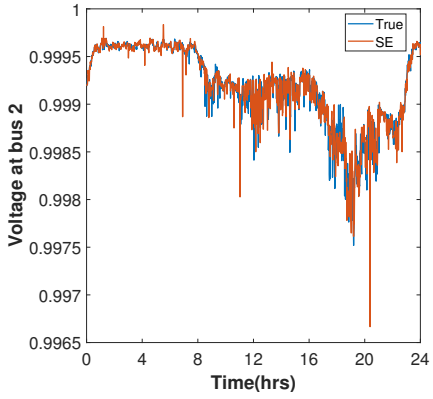

(c) 100% Pseudo-measurements

Figure 6.4: NR Power flow and State Estimation voltage comparision

The voltages correspond to each minute of the entire day for different percentages of real measurement availability and plotted as shown in figure 6.4. The selection of pseudo-measurements for the 50% case is done randomly by eliminating the real measurements from half of the nodes considered and replacing them with the pseudo-measurements. The x-axis represents the 24 hours in a day and the y-axis gives information about the estimated and true values of voltage states compared against each other. It can be concluded from these plots that the pattern followed by the estimated values is similar to that of the true values obtained from Newton Raphson PF. These plots alone do not justify in how similar the overlapping plots are. For better assessment, the plots in figure 6.4 are plotted as scatter plots as shown in figure 6.5 with the x-axis representing the voltage values obtained from WLS state estimation algorithm and the y-axis representing Newton-Raphson PF values.

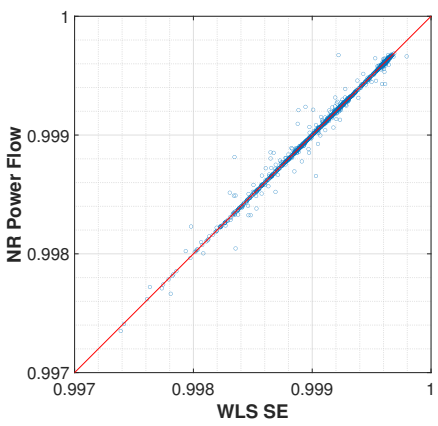

(a) 0% Pseudo-measurements

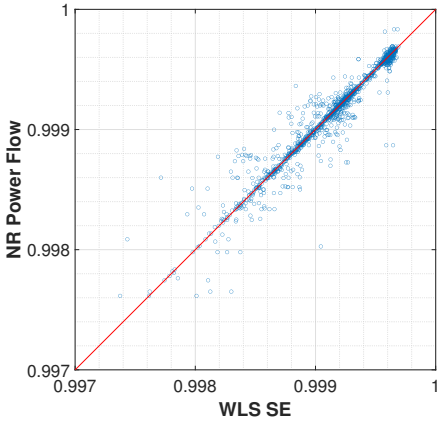

(b) 50% Pseudo-measurements

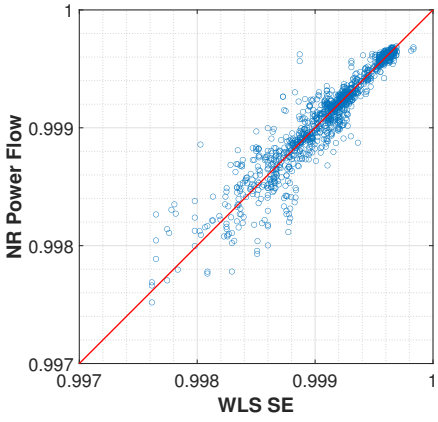

(c) 100% Pseudo-measurements

Figure 6.5: Scatter plots of voltages at bus 2

In the figure 6.5, the red line indicates the position of points in case of perfect estimation (line passing through the center representing **y=x**).

As seen, for the 0% pseudo-measurement case, most of the points lie on this line which is a good sign as the initial barrier has been overcome that proves that the algorithm does work for an ideal scenario. Few of the anomalies could be due to assumptions considered that the measurements are not correlated to each other in any sense.

As the percentage of pseudo-measurements increases, a deviation is observed away from this line. This is because the points are observed to be seen diverging because of an increase in the uncertainty in the input and hence the state estimation algorithm does not necessarily always spit the exact same value as expected. Inspite of this, from figure 6.3 it is seen that the error in measurements is less than 4% even in the case of 100% pseudo-measurements as input to the SE algorithm.

The computation time of the algorithm increases with an increase in pseudo-measurements included which is logical as the complexity of the problem has elevated. It is observed that for this particular case, when 100% pseudo-measurements are used, the computation time is about 1.9 times slower than the case when no pseudo-measurements are used. Also, the number of iterations required for the solution to converge at every minute varies and increases with increase in pseudo-measurements used. It is observed that on an average the algorithm requires around 4 iterations more to converge in the case of 100% pseudo-measurement case when compared with 0% pseudo-measurement case.

6.3.3. POWER FLOW

Similar to the absolute mean error plots in figure 6.3, the power flow errors are compared for different percentage of pseudo-measurements.

A small deviation in the voltage magnitude can have adverse effect on the power flows. It is imperative to keep an eye on how the power flows vary with the change in inputs. For this very reason, cumulative probability mean errors of power flows for all the branches is plotted as shown in figure 6.6.

For the case with 0% pseudo-measurements, it is seen that the errors are quite low. In the case with 50% pseudo-measurements,the maximum error that occurs is around 2%. In the case of 100% pseudo-measurements, it is observed that the error is less than 3% for a vast majority of power flows.

This implies that the mean errors of power flows increases for all the branches with larger injection of pseudo data. For this very reason, it is important to provide accurate inputs to the SE algorithm in terms of the mean and variance of pseudo-measurements especially to obtain good quality estimates.

In the event of availability of voltage measurements at few of the nodes, it is highly probable that better quality of output can be obtained due to a familiarity of few states. This is further verified with the second study system considered.

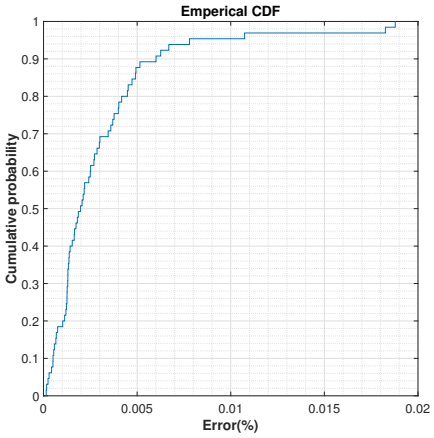

(a) 0% Pseudo-measurements

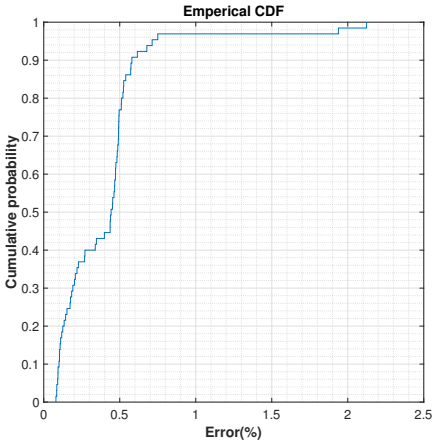

(b) 50% Pseudo-measurements

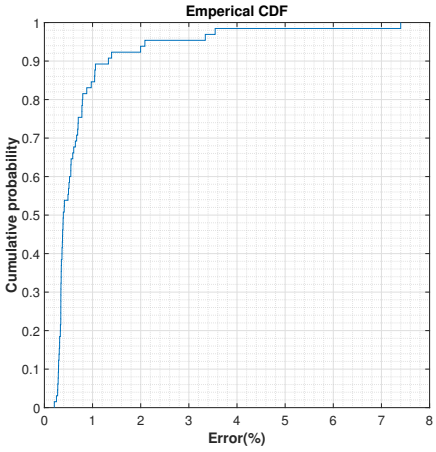

(c) 100% Pseudo-measurements

Figure 6.6: Mean Error probability of power flows in the network

6.4. NETWORK 2 WITH MEASURING DEVICES DATA

The Network 2 shown in figure 4.7 is the second case considered. This network is a part of a large grid in a region of the Netherlands that belongs to the network operator Stedin B.V. The measuring devices data at few of the load points is provided and for the rest of the points, where measuring device is not available, load profiles over the

whole year which have been previously collected by the DSO are available. The resolution of available measurements is five minutes apart. The pseudo-measurements are generated from the load profiles provided over the entire year for the buses which lack measuring devices data as explained in section 5.2.

The nodes that require pseudo-measurements are TL8, TL10, TL11, TL12, TL13 and the Load. For the other nodes the power injections and voltage magnitudes at few of them are available.

The state estimation algorithm is implemented for a duration of thirty days for the network. The estimation is done with two scenarios; the first one being without any voltage magnitude measurements considered and the second one with few voltage magnitude measurements considered as inputs. Significant difference in the quality of estimates is observed in these two scenarios.

6.4.1. WITHOUT VOLTAGE MEASUREMENTS

The network is shown in figure 6.7 with the highlighted node in red being the voltage bus i.e., bus 20 (TL7) for which the plot shown in figure 6.8 corresponds to. Multiple simulations are run for the entire month and the obtained values from state estimation are compared with the already available data from the measuring device (smart meter for a group of LV networks) for the same time period. In this scenario, no voltage magnitude measurements available are considered to perform state estimation. Only the power injections (at all nodes) are taken as inputs.

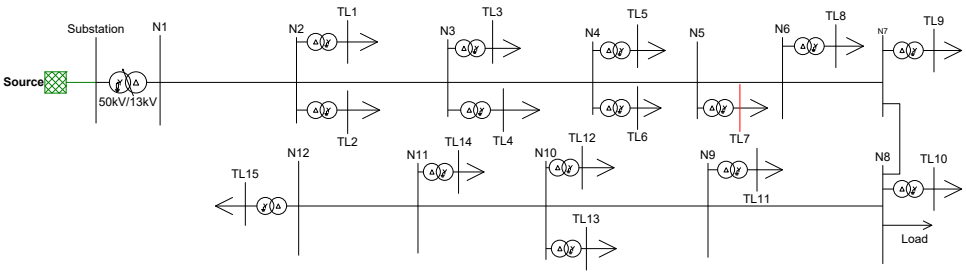

Figure 6.7: Stedin B.V network indicating the node where analysis is done

Figure 6.8 shows the state estimated voltage values over a month against the voltage from the measuring device data and most of them lie in close proximity as far as the similarity is considered. Similar to this, the other buses exhibit analogous characteristics.

The absolute mean error percentage for each of the instances is also plotted for bus 20 (TL7) in an emperical cumulative probability density plot. From this plot, it is further observed that the error is quite low and the algorithm is indeed effective

for networks with measuring device data.

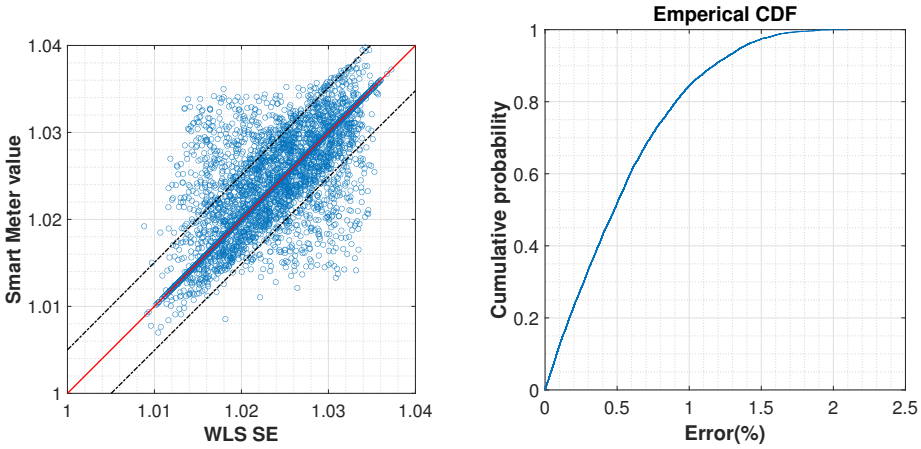

(a) Scatter plot of actual value vs estimated value

(b) Absolute mean error percentage ECDF

Figure 6.8: Voltage comparision and error probability of voltage state of bus 20

6.4.2. WITH VOLTAGE MEASUREMENTS

Further analysis is done taking into consideration few of the voltage magnitudes data from the measuring devices and state estimation is performed on the network. The nodes whose voltage magnitudes are taken as input (TL1, TL4 and TL9) are shown in figure 6.9 indicated by the circles in green.

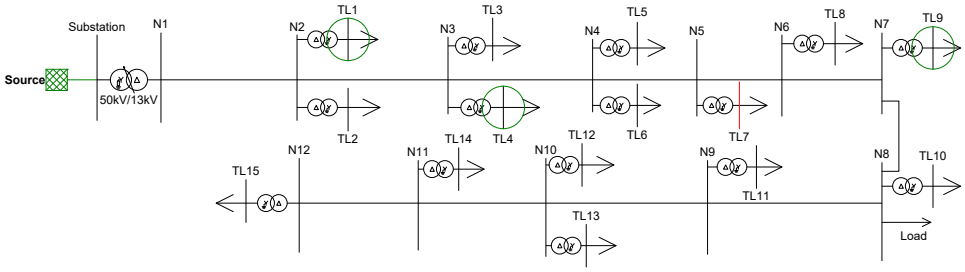

Figure 6.9: Stedin B.V network indicating the nodes where additional measurements are added

The scatter plot in figure 6.10 indicates the closeness of the state estimation algorithm value in comparision to the measuring device (smart meter for a group of LV networks) value. It is observed that the similarity of values increases significantly as compared to the previous case. This is due to the fact that the inputs when consist of

voltage measurements which are the states that need to be estimated, it is obvious that there is more clarity of the problem in hand for the state estimator. This therefore helps in attaining a closer output for the estimates than the case in which only power injections are used.

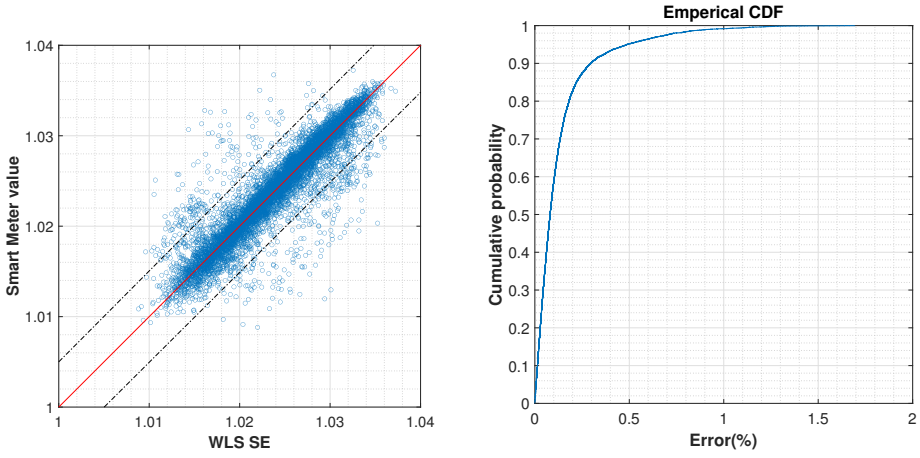

(a) Scatter plot of actual value vs estimated value

(b) Absolute mean error percentage ECDF

Figure 6.10: Voltage comparision and error probability of voltage state of bus 20

The absolute mean error also decreases which is due to the fact that taking voltages as input measurements increases accuracy. A slight change in voltage tends to have significant effect on the power flows and other related quantities. With the voltage magnitude already known at few of the nodes, the subsequent quantities which are iteratively used to determine the system state drastically improve and hence better results are obtained.

This shows that with consideration of voltages which are known at few points in the grid, a very huge boost is obtained to the algorithm. The estimated states most likely correspond to more accurate system states. This implies that it is possible to obtain other quantities in the grid and corresponds to the correct value more closely.

6.5. CONCLUSIONS DERIVED

From the analysis performed, the following implications are arrived at :

- With increase in usage of pseudo-measurement data, the estimated states do not converge as accurately as in cases with lesser pseudo-measurement injections.

- A small offset in voltage state can result in a large deviation in the power flows. This therefore relies on the input quality provided to the algorithm.
- The type and quality of input measurements used to determine the system states has a large effect on the accuracy.

7

CONCLUSION

This chapter gives a summary of the work done along with the answers to the research questions and few recommendations for future work.

7.1. SUMMARY

The importance of a DSSE and the issues associated with it have been identified to further identify the suitable algorithm to address the shortcomings.

The first area that has been focused upon is to identify the suitable state estimation algorithm for the distribution network. An in depth literature study has been done to identify all the plausible options which were deemed suitable. As is in the case of distribution networks, the measurements available are sparse and this further narrows down the list of estimators that can actually be used. To make the distribution networks observable, pseudo-measurements play an important role and the modelling of these are explored in Chapter 5. These are derived from historical load profile data and customer data available to the DSO and therefore are stochastic in nature. To identify the most suitable algorithm, statistical measures like bias and consistency were checked. With all the tests performed and relevant literature, it is concluded that WLS is the best fit.

The working of WLS algorithm on the networks using synthetic data and measuring devices data is verified in Chapter 6. The algorithm is implemented on the Dutch MV networks which are unique considering they are mostly comprised of underground cables. ALPG tool used here can be used to test future power grids before upgrading them. This is handy because before even going for costly upgrades, the feasibility of the system can be determined using this tool and the WLS algorithm. On the other hand, with the help of Stedin's data, the effect of change in type of input measurements could be simulated and observed.

The research questions indicated in Chapter 1 are answered in the upcoming section based on the work done in this thesis.

7.2. RESEARCH QUESTIONS

Which State Estimation Method(s) are suitable to be applied for the distribution networks across Netherlands?

A lot of potential DSSE algorithms have been explored in Chapter 2. Advantages and disadvantages of these algorithms have been compared with each other. Based on the results of this comparison and the advantages WLS algorithm possesses in static state estimation of MV networks, this algorithm has been selected for implementation.

How to adapt the state estimation algorithm selected for distribution grid?

The state estimation algorithms were initially formulated for transmission networks based on high redundancies in the grid measurements. Over time, with the growth in distribution networks DSSE came into play to deal with the uncertainty inherent to these networks. The algorithms used for transmission have been proved to be effective in the past provided the network considered is observable. Distribution networks have much less measurements available, which makes state estimation significantly more difficult. Appropriate choice of measurements weights and proper formulation of pseudo-measurements is necessary in this case in order to help the algorithm to efficiently deal with the problem at hand and ensure high accuracy.

What are the mathematical assumptions to be considered in order to formulate the pseudo measurements?

The load data is assumed to be normally distributed based on central limit theorem which is verified in [33] for large number of households and it is the case in this project. The pattern of the load profiles has been observed for a similar time instant spanning over a large number of days or profiles to form this normally distributed data. In the event of missing data or lack of measurements, this distribution is employed to select a value depending on the time instance of the day in order to make the system observable and also select the corresponding weight for the measurements as an input to the WLS algorithm. It is assumed that there is no bad data in any of the scenarios.

How does the state estimation algorithm perform with varying levels of redundancy in measurements?

Another interesting research question stems how the availability of measurements affects the estimated outputs. As expected with decrease in redundancy, the accuracy decreases too but the question lies about which measurements have higher probability of giving accurate results.

- An anonymized real-life distribution network with 65 buses is considered and power injections at various nodes are taken as input. Different cases are considered by varying the percentage of pseudo-measurements. The availability of active power injections coupled with the assumptions helps drive towards convergence of the solution but it is observed that an increase in percentage of pseudo-measurements affects the power flows in the network too.
- The other network considered is a part of Stedin's in the Netherlands. Data from measuring devices are considered and it is observed that with the inclusion of more measurements especially that of voltage, increases the accuracy by a large margin which in turn reflects in all corresponding measurements like power flows in the network. It can be concluded that having more measurements especially that of voltage tends to increase the accuracy of estimated states.

7.3. RECOMMENDATIONS FOR FUTURE WORK

During the course of the project, several suggestions have been encountered to expand the scope of research. Few of them are as follows:

- The distribution networks considered are assumed to be three phase balanced. Hence, three phase computation studies have not been performed but the methodology explained here is generic which can be extended to unbalanced phase studies.
- Better voltage assumptions can be taken at the nodes rather than a flat start to reduce the errors in power flow. This can be done if additional data is provided for the measuring devices from the DSOs or a better estimate from historical data with respect to the measured output data at the nodes. The upside to this is the convergence rate can increase reducing the computation time.
- Probability density functions of LV loads representing equivalents of LV distribution network might have more complex shape than normal Gaussian distirbution. In this case Gaussian Mixture models can be employed. The integration of Gaussian Mixture model into WLS state estimation framework can be the subject of future research.

BIBLIOGRAPHY

[1] M. F. Akorede, H. Hizam, and E. Pouresmaeil, "Distributed energy resources and benefits to the environment," *Renewable and Sustainable Energy Reviews*, vol. 14, no. 2, pp. 724–734, Feb. 2010, ISSN: 13640321. DOI: 10.1016/j.rser.2009.10.025.

[2] *Global Renewables Outlook: Energy Transformation 2050*, 2020th ed. International Renewable Energy Agency (IRENA), ISBN: 978-92-9260-238-3. [Online]. Available: https://www.irena.org/publications.

[3] *Energy report transition to sustainable energy*, 2016. [Online]. Available: https://www.government.nl/topics/renewable-energy/documents/reports/2016/04/28/energy-report-transition-tot-sustainable-energy.

[4] "North sea wind power hub programme," North Sea Wind Power Hub Programme. (), [Online]. Available: https://northseawindpowerhub.eu/.

[5] C. EJ(Edward), "Distribution grid operation including distributed generation: impact on grid protection and the consequences of fault ride-through behavior," Publisher: Technische Universiteit Eindhoven, Ph.D. dissertation, 2010. DOI: 10.6100/IR676122.

[6] R. Singh, "State estimation in power distribution network operation," Publisher: Imperial College of London, Ph.D. dissertation, 2009. DOI: 10.25560/5468.

[7] G. Hoogsteen, "A cyber-physical systems perspective on decentralized energy management," ISBN: 9789036544320, Ph.D. dissertation, University of Twente, Enschede, The Netherlands, Dec. 8, 2017. DOI: 10.3990/1.9789036544320.

[8] G. Hoogsteen, A. Molderink, J. L. Hurink, and G. J. Smit, "Generation of flexible domestic load profiles to evaluate demand side management approaches," in *2016 IEEE International Energy Conference (ENERGYCON)*, Leuven, Belgium: IEEE, Apr. 2016, pp. 1–6, ISBN: 978-1-4673-8463-6. DOI: 10.1109/ENERGYCON.2016.7513873.

[9] F. Schweppe and J. Wildes, "Power system static-state estimation, part i: Exact model," *IEEE Transactions on Power Apparatus and Systems*, vol. PAS-89, no. 1, pp. 120–125, Jan. 1970, ISSN: 0018-9510. DOI: 10.1109/TPAS.1970.292678.

[10] F. C. Schweppe and D. B. Rom, "Power system static-state estimation, part II: Approximate model," *IEEE TRANSACTIONS ON POWER APPARATUS AND SYSTEMS*, p. 6, 1970. DOI: 10.1109/TPAS.1970.292679.

[11] F. C. Schweppe, "Power system static-state estimation, part III: Implementation," p. 6, DOI: 10.1109/TPAS.1970.292680.

[12] E. Manitsas, R. Singh, B. Pal, and G. Strbac, "Modelling of pseudo-measurements for distribution system state estimation," *CIRED Seminar 2008: SmartGrids for Distribution*, 2008. DOI: 10.1049/ic:20080447.

[13] P. Rousseeuw, "Least median of squares regression," *Journal of the American Statistical Association*, vol. 79, Dec. 1984.

[14] D. L. Massart, L. Kaufman, P. J. Rousseeuw, and A. Leroy, "Least median of squares: A robust method for outlier and model error detection in regression and calibration," *Analytica Chimica Acta*, vol. 187, pp. 171–179, 1986, ISSN: 00032670. DOI: 10.1016/S0003-2670(00)82910-4.

[15] L. Mili, M. Cheniae, and P. Rousseeuw, "Robust state estimation of electric power systems," *IEEE Transactions on Circuits and Systems I: Fundamental Theory and Applications*, vol. 41, no. 5, pp. 349–358, May 1994, ISSN: 10577122. DOI: 10.1109/81.296336.

[16] M. Gol and A. Abur, "LAV based robust state estimation for systems measured by PMUs," *IEEE Transactions on Smart Grid*, vol. 5, no. 4, pp. 1808–1814, Jul. 2014, ISSN: 1949-3053, 1949-3061. DOI: 10.1109/TSG.2014.2302213.

[17] L. Mili, M. Cheniae, N. Vichare, and P. Rousseeuw, "Robust state estimation based on projection statistics [of power systems]," *IEEE Transactions on Power Systems*, vol. 11, no. 2, pp. 1118–1127, May 1996, ISSN: 08858950. DOI: 10.1109/59.496203.

[18] J. Zhao, G. Zhang, M. L. Scala, and Z. Wang, "Enhanced robustness of state estimator to bad data processing through multi-innovation analysis," *IEEE Transactions on Industrial Informatics*, vol. 13, no. 4, pp. 1610–1619, Aug. 2017, ISSN: 1551-3203, 1941-0050. DOI: 10.1109/TII.2016.2626782.

[19] P. J. Huber, *Robust statistics*, ser. Wiley series in probability and mathematical statistics. New York: Wiley, 1981, 308 pp., ISBN: 978-0-471-41805-4.

[20] U. Kuhar, M. Pantos, G. Kosec, and A. Svigelj, "The impact of model and measurement uncertainties on a state estimation in three-phase distribution networks," *IEEE Transactions on Smart Grid*, vol. 10, no. 3, pp. 3301–3310, May 2019, ISSN: 1949-3053, 1949-3061. DOI: 10.1109/TSG.2018.2823398.

[21] K. Dehghanpour, Z. Wang, J. Wang, Y. Yuan, and F. Bu, "A survey on state estimation techniques and challenges in smart distribution systems," *IEEE Transactions on Smart Grid*, vol. 10, no. 2, pp. 2312–2322, Mar. 2019, ISSN: 1949-3053, 1949-3061. DOI: 10.1109/TSG.2018.2870600. arXiv: 1809.00057.

[22] R. Jabr, B. Pal, and R. Singh, "Choice of estimator for distribution system state estimation," *IET Generation, Transmission & Distribution*, vol. 3, no. 7, pp. 666–678, Jul. 1, 2009, ISSN: 1751-8687, 1751-8695. DOI: 10.1049/iet-gtd.2008.0485.

[23] M. Baran and A. Kelley, "State estimation for real-time monitoring of distribution systems," *IEEE Transactions on Power Systems*, vol. 9, no. 3, pp. 1601–1609, Aug. 1994, ISSN: 08858950. DOI: 10.1109/59.336098.

[24] D. A. Haughton and Heydt, "A linear state estimation formulation for smart distribution systems," *IEEE Transactions on Power Systems*, vol. 28, no. 2, pp. 1187–1195, May 2013, ISSN: 0885-8950, 1558-0679. DOI: 10.1109/TPWRS.2012.2212921.

[25] Youman Deng, Ying He, and Boming Zhang, "A branch-estimation-based state estimation method for radial distribution systems," *IEEE Transactions on Power Delivery*, vol. 17, no. 4, pp. 1057–1062, Oct. 2002, ISSN: 0885-8977. DOI: 10.1109/TPWRD.2002.803800.

[26] C. Lu, J. Teng, and W.-H. Liu, "Distribution system state estimation," *IEEE Transactions on Power Systems*, vol. 10, no. 1, pp. 229–240, Feb. 1995, ISSN: 08858950. DOI: 10.1109/59.373946.

[27] M. Baran and A. Kelley, "A branch-current-based state estimation method for distribution systems," *IEEE Transactions on Power Systems*, vol. 10, no. 1, pp. 483–491, Feb. 1995, ISSN: 08858950. DOI: 10.1109/59.373974.

[28] M. Baran, "Branch current based state estimation for distribution system monitoring," in *2012 IEEE Power and Energy Society General Meeting*, San Diego, CA: IEEE, Jul. 2012, pp. 1–4, ISBN: 978-1-4673-2729-9 978-1-4673-2727-5 978-1-4673-2728-2. DOI: 10.1109/PESGM.2012.6344841.

[29] M. E. Baran, J. Jung, and T. E. McDermott, "Including voltage measurements in branch current state estimation for distribution systems," in *2009 IEEE Power & Energy Society General Meeting*, Calgary, Canada: IEEE, Jul. 2009, pp. 1–5, ISBN: 978-1-4244-4241-6. DOI: 10.1109/PES.2009.5275479.

[30] H. Wang and N. Schulz, "A revised branch current-based distribution system state estimation algorithm and meter placement impact," *IEEE Transactions on Power Systems*, vol. 19, no. 1, pp. 207–213, Feb. 2004, ISSN: 0885-8950. DOI: 10.1109/TPWRS.2003.821426.

[31] A. Angioni, T. Schlosser, F. Ponci, and A. Monti, "Impact of pseudo-measurements from new power profiles on state estimation in low-voltage grids," *IEEE Transactions on Instrumentation and Measurement*, vol. 65, no. 1, pp. 70–77, Jan. 2016, ISSN: 0018-9456, 1557-9662. DOI: 10.1109/TIM.2015.2454673.

[32] J. Nazarko and Z. Styczynski, "Application of statistical and neural approaches to the daily load profiles modelling in power distribution systems," in *1999 IEEE Transmission and Distribution Conference (Cat. No. 99CH36333)*, New Orleans, LA, USA: IEEE, 1999, 320–325 vol.1, ISBN: 978-0-7803-5515-6. DOI: 10.1109/TDC.1999.755372.

[33] Y. Xiang, "Operation of future medium voltage distribution grids: Application of statistical methods for state estimation and fault location," OCLC: 8087211698, Ph.D. dissertation, Technische Universiteit Eindhoven, 2015.

[34] A. Kewo, P. D. K. Manembu, and P. S. Nielsen, "Synthesising residential electricity load profiles at the city level using a weighted proportion (wepro) model," *Energies*, vol. 13, no. 14, p. 3543, Jul. 9, 2020, ISSN: 1996-1073. DOI: 10.3390/en13143543.

[35] N. Pflugradt and U. Muntwyler, "Synthesizing residential load profiles using behavior simulation," *Energy Procedia*, vol. 122, pp. 655–660, Sep. 2017, ISSN: 18766102. DOI: 10.1016/j.egypro.2017.07.365.

[36] J. Widén, M. Lundh, I. Vassileva, E. Dahlquist, K. Ellegård, and E. Wäckelgård, "Constructing load profiles for household electricity and hot water from time-use data—modelling approach and validation," *Energy and Buildings*, vol. 41, no. 7, pp. 753–768, Jul. 2009, ISSN: 03787788. DOI: 10.1016/j.enbuild.2009.02.013.

[37] A. Abur and A. Gómez Expósito, *Power system state estimation: theory and implementation*, ser. Power engineering. New York, NY: Marcel Dekker, 2004, 327 pp., OCLC: ocm55070738, ISBN: 978-0-8247-5570-6. DOI: 10.1201/9780203913673.

[38] D. Kothari and I. Nagrath, *Modern Power System Analysis*. New Delhi: Tata McGraw- Hill, 2004, ISBN: 978-0-07-107775-0.

[39] F. L. Lewis, "Optimal and robust estimation: With an introduction to stochastic control theory, second edition," p. 547,

[40] A. B. Younes and J. Turner, "Generalized least squares and newton's method algorithms for nonlinear root-solving applications," *The Journal of the Astronautical Sciences*, vol. 60, no. 3, pp. 517–540, Dec. 2013, ISSN: 0021-9142, 2195-0571. DOI: 10.1007/s40295-015-0071-z.

[41] A. K. Kaw, *Introduction to Matrix Algebra*. Autarkaw, ISBN: 978-0-615-25126-4. [Online]. Available: http://ckw.phys.ncku.edu.tw/public/pub/Notes/Mathematics/LinearAlgebra/Web/matrixalgebra.pdf.

[42] "Introduction to numerical methods," in *Introduction to Numerical Methods*. [Online]. Available: https://learn.lboro.ac.uk/archive/olmp/olmp_resources/pages/workbooks_1_50_jan2008/Workbook30/30_4_mtrx_norms.pdf.

[43] I. S. Gradshteĭn, I. M. Ryzhik, and A. Jeffrey, *Table of integrals, series, and products*, 7th ed. Amsterdam ; Boston: Academic Press, 2007, 1171 pp., ISBN: 978-0-12-373637-6. DOI: 10.1016/C2009-0-22516-5.

[44] S. Bhattacharyya, Z. Wang, J. F. G. Cobben, J. M. A. Myrzik, and W. L. Kling, "Analysis of power quality performance of the dutch medium and low voltage grids," *2008 13th International Conference on Harmonics and Quality of Power*, p. 6, DOI: 10.1109/ICHQP.2008.4668800.

[45] "Energie in cijfers | hoofdstuk 1: Kerngegevens energienetten," Energie in cijfers. (), [Online]. Available: https://energiecijfers.info/hoofdstuk-1/.

[46] "Phase to phase – netten voor distributie van elektriciteit." (), [Online]. Available: https://phasetophase.nl/boek/index.html.

[47] S. Mokey. “5 important SCADA components for data collection and management,” Digitronik Labs. (Feb. 14, 2019), [Online]. Available: https://www.digitroniklabs.com/blog/scada-components-data-collection-management/.

[48] “Open power system data – a platform for open data of the european power system.” (), [Online]. Available: https://open-power-system-data.org/.

[49] N. Blaauwbroek, D. Kuiken, P. Nguyen, H. Vedder, M. Roggenkamp, and H. Slootweg, “Distribution network monitoring: Interaction between EU legal conditions and state estimation accuracy,” *Energy Policy*, vol. 115, pp. 78–87, Apr. 2018, ISSN: 03014215. DOI: 10.1016/j.enpol.2017.12.041.

[50] T. W. Anderson, *An introduction to multivariate statistical analysis*, 3rd ed, ser. Wiley series in probability and statistics. Hoboken, N.J: Wiley-Interscience, 2003, 721 pp., ISBN: 978-0-471-36091-9.

[51] “Values of the chi-squared distribution.” (), [Online]. Available: https://www.medcalc.org/manual/chi-square-table.php.

A

Conversion of Vision file to Matpower file

Since MATLAB is used to formulate and test the State Estimation algorithm, the .vnf file which is created in Vision Network Analysis that contains the network data is converted to Matpower format using a tool developed by Phase to Phase BV.

Figure A.1: Vision to MATPower converter UI

The interface of the tool is shown in figure above. The .vnf file of the network

to be converted is opened and then the option to convert to Matpower is selected. Then the option to select S_{nom} (10 MVA) and the frequency (50 Hz) is presented. Upon selecting the corresponding values, the file is converted to Matpower format. The loads are represented in MW and MVar format but the line impedances and resistances are in per unit values.

B

Network 1 data

Table B.1: Network 1 Bus data

Bus	Bus Type	Base Voltage (kV)	Bus Name
1	Slack	10.6	Substation
2	PQ	10.6	K1
3	PQ	10.6	K2
4	PQ	10.6	K3
5	PQ	10.6	K4
6	PQ	10.6	K5
7	PQ	10.6	K6
8	PQ	10.6	K7
9	PQ	10.6	K8
10	PQ	10.6	K9
11	PQ	10.6	K10
12	PQ	10.6	K11
13	PQ	10.6	K12
14	PQ	10.6	K13
15	PQ	10.6	K14
16	PQ	10.6	K15
17	PQ	10.6	K16
18	PQ	10.6	K17
19	PQ	10.6	K18
20	PQ	10.6	K19
21	PQ	10.6	K20
22	PQ	10.6	K21
23	PQ	10.6	K22
24	PQ	10.6	K23
25	PQ	10.6	K24

Continued on next page

Table B.1 – continued from previous page

Bus	Bus Type	Base Voltage(kV)	Bus Name
26	PQ	10.6	K25
27	PQ	10.6	K26
28	PQ	10.6	K27
29	PQ	10.6	K28
30	PQ	10.6	K29
31	PQ	10.6	K30
32	PQ	10.6	K31
33	PQ	10.6	K32
34	PQ	0.4	T1
35	PQ	0.4	T2
36	PQ	0.4	T3
37	PQ	0.4	T4
38	PQ	0.4	T5
39	PQ	0.4	T6
40	PQ	0.4	T7
41	PQ	0.4	T8
42	PQ	0.4	T9
43	PQ	0.4	T10
44	PQ	0.4	T11
45	PQ	0.4	T12
46	PQ	0.4	T13
47	PQ	0.4	T14
48	PQ	0.4	T15
49	PQ	0.4	T16
50	PQ	0.4	T17
51	PQ	0.4	T18
52	PQ	0.4	T19
53	PQ	0.4	T20
54	PQ	0.4	T21
55	PQ	0.4	T22
56	PQ	0.4	T23
57	PQ	0.4	T24
58	PQ	0.4	T25
59	PQ	0.4	T26
60	PQ	0.4	T27
61	PQ	0.4	T28
62	PQ	0.4	T29
63	PQ	0.4	T30
64	PQ	0.4	T31
65	PQ	0.4	T32

Table B.2: Network 1 Line data

From Bus	To Bus	R (p.u.)	X (p.u.)	B (p.u.)
1	21	0.046253293	0.014855643	0.002325070
21	22	0.023258277	0.005976148	0.000979192
22	23	0.003085440	0.000788181	0.000129618
23	24	0.003114009	0.000795479	0.000130818
24	25	0.011638750	0.003094874	0.000496374
25	26	0.014198736	0.003627091	0.000596481
26	27	0.008113564	0.002072624	0.000340847
27	28	0.006770826	0.001729619	0.000284439
28	29	0.002828320	0.000722499	0.000118816
29	30	0.008056426	0.002058028	0.000338446
1	2	0.090042809	0.027835707	0.004272654
2	3	0.021317640	0.005864454	0.000921126
3	4	0.012377447	0.003911089	0.000565736
4	33	0.011571111	0.003635546	0.000527613
32	33	0.013304735	0.003669722	0.000575479
31	32	0.015652456	0.003003293	0.000434424
30	31	0.011350214	0.003093628	0.000488678
3	5	0.008028658	0.003393556	0.000558076
5	6	0.007685030	0.001987095	0.000313349
6	7	0.006313724	0.001632520	0.000257435
7	8	0.017455589	0.004513439	0.000711732
8	9	0.011427554	0.002954788	0.000465946
9	10	0.011484692	0.002969562	0.000468276
10	11	0.005885190	0.001521716	0.000239962
11	33	0.013783998	0.004196422	0.000616355
1	12	0.031505073	0.010283909	0.001694066
12	13	0.007476682	0.002180936	0.000330645
13	14	0.015506408	0.003405660	0.000508234
14	15	0.011108580	0.003510146	0.000507740
15	16	0.003767444	0.001026166	0.000162163
16	17	0.005913403	0.001868548	0.000270284
17	18	0.007354041	0.001955411	0.000313631
18	19	0.009656283	0.002466714	0.000405655
19	20	0.007827875	0.001999644	0.000328845
20	27	0.019912513	0.005086686	0.000836514
11	20	0.013430313	0.005060698	0.001080783

C

Network 2 data

Table C.1: Network 2 Bus data

Bus	Bus Type	Base Voltage (kV)	Bus Name
1	PQ	13	N1
2	Slack	50	Grid
3	PQ	13	N2
4	PQ	13	N3
5	PQ	13	N4
6	PQ	13	N5
7	PQ	13	N6
8	PQ	13	N7
9	PQ	13	N8
10	PQ	13	N9
11	PQ	13	N10
12	PQ	13	N11
13	PQ	13	N12
14	PQ	0.4	TL2
15	PQ	0.4	TL1
16	PQ	0.4	TL4
17	PQ	0.4	TL3
18	PQ	0.393	TL6
19	PQ	0.393	TL5
20	PQ	0.393	TL7
21	PQ	0.420	TL8
22	PQ	0.4	TL9
23	PQ	0.420	TL10
24	PQ	0.4	TL11
25	PQ	0.420	TL13

Continued on next page

Table C.1 – continued from previous page

Bus	Bus Type	Base Voltage(kV)	Bus Name
26	PQ	0.420	TL12
27	PQ	0.4	TL14
28	PQ	0.393	TL15

Table C.2: Network 2 Line data

From Bus	To Bus	R (p.u.)	X (p.u.)	B (p.u.)
1	3	0.005802094	0.002846778	0.000774802
3	4	0.007459303	0.003085439	0.000882261
4	5	0.005155019	0.002132303	0.000609718
5	6	0.007423092	0.003070461	0.000877978
6	7	0.011506756	0.005419386	0.001316471
9	10	0.028401428	0.011747863	0.003359223
7	8	0.005331226	0.002510659	0.000609952
8	9	0.002422555	0.001002057	0.000286531
10	11	0.008729043	0.003735990	0.001014104
12	13	0.028511369	0.004288424	0.000690116
11	12	0.008064389	0.003456270	0.000936192